

LIBRARY
Michigan State
University

PLACE IN RETURN BOX to remove this checkout from your record.
TO AVOID FINES return on or before date due.
MAY BE RECALLED with earlier due date if requested.

DATE DUE	DATE DUE	DATE DUE

**CELL CULTURE AT THE LIQUID-LIQUID INTERFACE: EFFECTS OF
FLUOROCARBON LAYER THICKNESS ON CELL GROWTH**

By

Victoria A. Sanocki

A THESIS

**Submitted to
Michigan State University
in partial fulfillment of the requirements
for the degree of**

MASTER OF SCIENCE

Department of Chemical Engineering

2004

ABSTRACT

CELL CULTURE AT THE LIQUID-LIQUID INTERFACE: EFFECTS OF FLUOROCARBON LAYER THICKNESS ON CELL GROWTH

By

Victoria A. Sanocki

This study assessed the effect of fluorocarbon layer thickness on the adsorption of proteins at the liquid-liquid interface, and on subsequent attachment, growth and differentiation of 3T3 fibroblasts cultured at that interface. Cells were grown at the interface between culture medium and fluorinert liquid FC-70 layers of 5 mm, 1 mm, and 0.5 mm. The interfaces were treated with either fibronectin (FN) or human serum albumin (HSA). Growth and proliferation improved as FC-70 layer thickness decreased, with the best growth on the 0.5 mm layer. Cell growth on the FN-treated interfaces was better than on the HSA-treated ones. The occurrence and size of cell-free gaps (or “lakes”) decreased with thickness, with the smallest cell-free areas occurring on the 0.5 mm FN-treated fluorocarbon layer. The adsorption of HSA and FN was also studied at the liquid-liquid interface, using total internal reflection fluorescence microscopy and fluorescence photobleaching recovery (TIRFM/FPR) on oil layers ranging in thickness from 4 μm to 50 μm . The fraction of irreversibly adsorbed proteins, g_0 , did not vary with thickness for either FN or HSA; however, FN had higher g_0 values than HSA in all cases. Taken together, the cell culture and TIRFM/FPR data suggest a sigmoidal behavior for the rate of cell growth as a function of fluorocarbon layer thickness, with cell density approaching some maximum value as the fluorocarbon layer becomes infinitely thin.

DEDICATION

To my parents, for all of their love and support.

ACKNOWLEDGMENTS

I wish to thank my major advisor, Dr. R. Y. Ofoli, for his guidance and support throughout my studies. I would also like to thank Drs. C. Chan and R. M. Worden for serving on my advisory committee, and for their suggestions.

I would especially like to thank Dr. Chan for generously donating cells and the use of her laboratory facilities for this project. Special thanks go to Srivatsan Kidambi for his invaluable help with cell culture and for answering all my questions about it. I would also like to thank Sachin Vaidya and Lavanya Parthasarathy for lending me their expertise on total internal reflection fluorescence microscopy and for being there to commiserate and offer advice when things did not go as expected.

I would like to thank my fiancé, Kevin Brown, for his love and for being there to encourage me and keep me going when I was feeling down. I would also like to thank my sisters, Ellen and Abigail Sanocki, for being there.

TABLE OF CONTENTS

LIST OF TABLES	vii
LIST OF FIGURES	viii
NOMENCLATURE.....	x
1. INTRODUCTION.....	1
1.1 Objective	5
2. LITERATURE REVIEW	6
2.1 Cell Culture at the Liquid-Liquid Interface.....	6
2.2 Total Internal Reflection Fluorescence	10
3. THEORETICAL CONSIDERATIONS.....	17
3.1 Total Internal Reflection	17
3.2 Fluorescence Photobleaching Recovery.....	18
4. EXPERIMENTAL MATERIALS AND TECHNIQUES	22
4.1 Materials.....	22
4.2 Experimental Methods	23
4.2.1 Cell Culture	23
4.2.1.1 Preparation of liquid-liquid interface.....	23
4.2.1.2 Growth Curves	23
4.2.2 TIRFM/FPR	24
4.2.2.1 TIRFM Apparatus	24
4.2.2.2 Procedure for Labeling Proteins.....	27
4.2.2.3 Beam Alignment and Microscope Focusing Procedure	28
4.2.2.4 Photobleaching	29
4.2.2.5 Data Analysis	29
5. RESULTS AND DISCUSSION.....	30
5.1 Cell Culture	30
5.2 TIRFM/FPR	43
6. SUMMARY AND CONCLUSIONS.....	51
7. SUGGESTIONS FOR FUTURE WORK.....	55

8.	APPENDICES.....	57
8.1	Appendix A: Physical Properties of FC-70.....	57
	Properties.....	57
8.2	Appendix B: Sigma Plot Output	58
9.	BIBLIOGRAPHY	60
9.1	General References.....	64

LIST OF TABLES

Table 1: TIRFM/FPR results for HSA. Data are presented \pm the standard error from regression.	47
Table 2: TIRFM/FPR results for FN. Data are presented \pm the standard error from regression.	47
Table 3: Physical properties of FC-70. Values are determined at 25 °C.	57

LIST OF FIGURES

- Figure 1.1: Schematics of cell culture at the liquid-liquid interface. We hypothesize that, as the fluorocarbon layer gets thinner, the liquid-liquid interface would become more stable on the solid substrate and promote better protein adhesion and subsequent cell attachment, growth and proliferation. 4
- Figure 3.1: Total internal reflection at an interface, induced by laser beam entering the interface at an angle exceeding the critical angle. The resulting evanescent wave decays exponentially with distance into the optically rarer medium..... 18
- Figure 4.1: The experimental set up for TIRFM. The double flat system (F) splits the beam into an intense photobleaching beam (pb) and a much weaker monitoring beam (m), and then recombines them to ensure that both beams are incident at the same spot on the interface. Mirrors (M) enable focusing of the beam into the sample cell²⁷. 25
- Figure 4.2: The experimental flow cell. Spin coating controls the thickness of the oil layer on the top slide. The entire oil-water assembly is approximately 800 μm thick. 27
- Figure 5.1: Growth curves for FN-treated FC-70-culture media interfaces. 'Untreated' refers to a 5 mm FC-70 layer on which FN was not adsorbed prior to the cell culture experiment. Lines do not represent models, but have been added to aid in visualizing trends. All cell count data were normalized against the initial seeding density. 32
- Figure 5.2: Cell behavior on 0.5 mm (A) and 1 mm (B) FN-treated FC-70 layers, after 3 days of incubation. There are only a few small cell-free gaps on the 0.5 mm layer (A). However, there is evidence of more protein layer rupture and aggregate formation (dark spot) on the 1 mm layer (B). The two images are of identical magnification..... 33
- Figure 5.3: Growth curves for HSA-culture media interfaces. 'Untreated' refers to a 5 mm thick FC-70 layer on which HSA was not adsorbed prior to the cell culture experiment. Lines have been added to aid in visualizing trends. All cell count data were normalized against the initial seeding density. 35

Figure 5.4: Cell behavior on 0.5 mm (A) and 1 mm (B) HSA-treated FC-70 layers, after 3 days of incubation. Cell growth in both cases is sparse. There are more and larger aggregates (dark spots) on the 1 mm layer (B)..... 36

Figure 5.5: Cell count as a function of fluorocarbon layer thickness for FN and HSA on Days 2 (top), 3 (middle), and 4 (bottom). Lines have been added to aid in visualizing trends. All cell count data were normalized against the initial seeding density. 37

Figure 5.6: Cell growth on 0.5 mm FC-70-culture media interfaces after 3 days of incubation for FN (A) and HSA (B). Cell growth on the FN-treated interface is clearly much more robust than on the HSA-treated interface. 38

Figure 5.7: Cells before (A) and after (B) 20 minutes of trypsin-EDTA treatment on 1 mm of FN-treated FC-70-medium interface. The cells have not rounded up after being treated with trypsin-EDTA, so they cannot be completely removed by trypsin-EDTA treatment. 40

Figure 5.8: Cells before (A) and after (B) 20 minutes of trypsin-EDTA treatment on 1 mm of HSA-treated FC-70-medium interface. Most of the cells have rounded up and are ready to be detached after trypsin-EDTA treatment. 41

Figure 5.9: Cells before (A) and after (B) 20 minutes of trypsin-EDTA treatment on polystyrene culture plate. All of the cells have rounded up and are ready to be removed from the plastic surface (B). 42

Figure 5.10: Sample fluorescence recovery curve for HSA adsorbed at an interface featuring a 6 μm oil layer. The fluorescence units are arbitrary (A.U.). The slow recovery of fluorescence after photobleaching is an indication that a large fraction of protein is bound irreversibly to the interface..... 44

Figure 5.11: Sample $g(t)$ data and regression fit for HSA on 6 μm oil layer. $g(t)$ is normalized from the fluorescence recovery curve (Figure 5.10). The single exponential model fits the data well, even at later times. 45

Figure 5.12: Most likely cell growth curve as a function of fluorocarbon layer thickness for FN on Day 3. The dashed line represents the most plausible cell growth profile, based on the combination of results from TIRFM/FPR and cell culture experiments. 50

NOMENCLATURE

θ	angle of incidence of laser beam
θ_c	critical angle
λ_0	wavelength of incident laser beam
$A(\mathbf{r}, z, t)$	bulk concentration of molecules
$[A]$	equilibrium bulk concentration of molecules
$B(\mathbf{r}, t)$	surface concentration of free binding sites
$[B]$	equilibrium surface concentration of free binding sites
$C(\mathbf{r}, t)$	surface concentration of bound molecules
$[C]$	equilibrium surface concentration of bound molecules
$C(\mathbf{r}, t)$	surface concentration of unbleached fluorescent molecules
d	penetration depth of the evanescent wave
D_A	bulk diffusion coefficient
EDTA	Ethylenediaminetetraacetic acid
\bar{F}	equilibrium pre-bleach fluorescence emission intensity
$F(0)$	fluorescence emission intensity immediately after photobleaching
$F(t)$	measured fluorescence emission intensity as a function of time
FITC	fluorescein-5-isothiocyanate (fluorescent dye)
FN	fibronectin
FPR	fluorescence photobleaching recovery
g_0	fraction of molecules that are irreversibly bound at the interface

g_i	fraction of molecules belonging to binding class i
HSA	human serum albumin
I_0	laser intensity at the interface ($z=0$)
$\mathcal{A}(\mathbf{r})$	dimensionless profile function
$I(z)$	intensity of evanescent wave at any depth z
k_1	surface adsorption rate
$k_2(i)$	surface desorption rate of molecule in class i
n_j	refractive index of media j
PMT	photomultiplier tube
Q	system constant
\mathbf{r}	radial position vector
t	time
TIRFM	total internal reflection fluorescence
z	depth coordinate into rarer media

1. INTRODUCTION

The purpose of cell culture is to produce, nurture and maintain viable cells outside of their original multicellular host organism. The behavior of the cells and how they are influenced by certain conditions can then be observed without interference from other systems or functions in the animal they were taken from. To keep it viable, the environment around the cultured cell must mimic the cell's original surroundings. Cells must be kept clean and fed in a setting that will promote growth, and potentially harmful byproducts of cellular activity must be removed from the environment. Culture media must be carefully formulated to provide the nutrients required for cell viability. For example, oxygen must diffuse through the culture media to reach cells. Too much culture medium may retard diffusion, and result in oxygen deprivation and eventually cell death. To this end, researchers have been perfecting culture media and techniques over the past century.

In 1907, Ross Harrison grew frog neural tissue in a sealed container filled with frog lymph¹. His experiments fostered more interest in maintaining cells and organs outside of animals for research purposes. Due to the desire to examine systems that better approximated humans, mammalian cells became the primary focus for many tissue culturists. Virology and cancer research further improved tissue culture by standardizing techniques and media, along with establishing many continuous cell lines for future research.

The standardization of procedures and media, along with the increased availability of cells for culture opened tissue culture up to many other applications and areas of research beyond cell biology. Cultured cells provide a source of DNA sequences and a means of determining the effects of transfected genes for gene therapy. Tissue culture decreases the need for animal experimentation in drug, cosmetic, and pollutant toxicity tests. Large-scale cell cultures, whether genetically altered or not, can lead to products such as insulin for the treatment of diseases. Tissue grafts and scaffolds seeded with cultured cells can be used to replace damaged tissue. Therefore, tissue culture is not just academic; it leads to products that can enhance the quality of life.

Tissue culture of adherent or anchorage-dependent cells has been traditionally carried out on solids, primarily glass or plastic. These solid substrates provide the support adherent cells need to grow and proliferate. The most commonly used plastic is polystyrene, which must be treated with γ irradiation, chemically, or with gas-plasma discharge to support cell growth¹. These treatments do not always produce uniform surfaces and the quality varies from manufacturer to manufacturer. In addition, some organic solvents erode polystyrene. Plastic or glass surfaces can also be treated with proteins such as fibrinogen or fibronectin to enhance cell growth. To be removed from the interface, cells must be treated with digestive enzymes like trypsin-ethylenediaminetetraacetic acid (EDTA) or be scraped off. These treatments can damage the cell. For example, scraping may cause cells to burst if too much force is applied. Alternatives to cell culture on a solid substrate have been used to avoid some of these problems.

An interesting but little used alternative for growing anchorage-dependent cells is to use a liquid-liquid interface, a technique Rosenberg² introduced in 1964. The lower phase is dense immiscible oil, typically a fluorocarbon, while the upper phase is a culture medium. The resulting interface provides support for cell growth, with cells growing on a layer of adsorbed interfacial proteins. However, since cells do not adhere to a liquid-liquid interface as strongly as they would to a solid-liquid interface, pipetting or centrifugation can be used to remove cells from the surface, resulting in little or no damage^{3,4}.

Fluorocarbons are usually the preferred hydrophobic substrate for cell culture at the liquid-liquid interface, because their properties make them ideal for that purpose. The medical field already employs them as blood substitutes and for short-term organ preservation⁵. They are chemically and biologically inert and are thermally stable. With a high solubility to respiratory gases, fluorocarbons can easily provide oxygen to cells⁵. Therefore, the supply of oxygen is not just limited to diffusion through the culture medium. Fluorocarbons can also be re-sterilized and reused.

Despite the advantages of fluorocarbons, there are some drawbacks to cell culture at the liquid-liquid interface. Purified fluorocarbons are often poor substrates for cell growth, because trace impurities generally improve protein adsorption at the interface and improve protein film quality, both of which are essential for ensuring the growth of anchorage-dependent cells⁶. However, some of these impurities may be toxic at high concentration. Much more care is required when handling cultures. For example, sloshing the oil may cause cells to detach and form aggregates. If the protein layer is

ruptured, large lake-like openings will form in the cell sheet⁷. The forces cells exert on the protein layer as they grow and proliferate may induce protein desorption from the interface or cause the protein layer to rupture, which leads to clump formation.

In this study, we hypothesized that decreasing the thickness of the fluorocarbon layer may provide a solution to the problem of protein layer rupture. When the thickness of the fluorocarbon layer is decreased, the liquid-liquid interface is brought closer to the underlying solid substrate (Figure 1.1), promoting stability of the liquid-liquid interface and anchoring it more securely to the solid substrate. This increased stability should lead to better anchoring of proteins upon adsorption at the interface, promote better cell growth and proliferation, and reduce the possibility of protein layer rupture and formation of lake-like openings in the cell sheet. The result is that cell growth characteristics will be similar to those on a solid surface, while still maintaining many of the benefits of cell culture at a liquid-liquid interface.

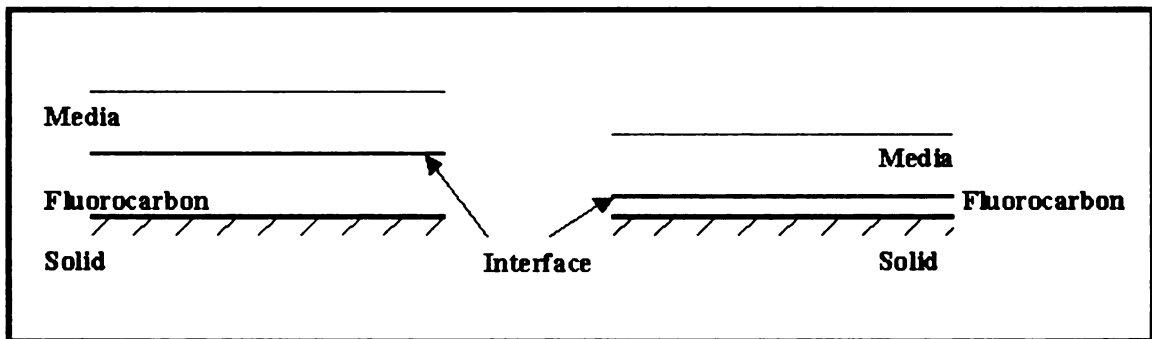


Figure 1.1: Schematics of cell culture at the liquid-liquid interface. We hypothesize that, as the fluorocarbon layer gets thinner, the liquid-liquid interface would become more stable on the solid substrate and promote better protein adhesion and subsequent cell attachment, growth and proliferation.

1.1 Objective

The objective of this study was to assess the effect of fluorocarbon layer thickness on the adsorption of proteins at the liquid-liquid interface, and on the attachment, growth and differentiation of cells cultured at the interface. The study focused on the following specific activities:

- Use of total internal reflection fluorescence microscopy and fluorescence photobleaching recovery (TIRFM/FPR) to study the irreversibility of protein adsorption at the oil-water interface as a function of oil layer thickness; and
- Use of growth curves to assess the effects of fluorocarbon layer thickness on cell attachment, growth, and proliferation at the interface.

Cells were cultured at fluorocarbon layers of varying thickness treated with either fibronectin or human serum albumin. Fibronectin is important for cellular adhesion, migration, and proliferation⁸. Human serum albumin, on the other hand, transports other substances in the blood, such as bile acids, drugs, toxins, and excess hormones and vitamins⁹. Human serum albumin is also known to decrease the adhesion of cells on solid substrata^{10,11}. The adsorption of these proteins at the liquid-liquid interface was studied directly with total internal reflection fluorescence microscopy, along with fluorescence photobleaching recovery, to determine the effects of oil layer thickness.

2. LITERATURE REVIEW

2.1 Cell Culture at the Liquid-Liquid Interface

Rosenberg² introduced the technique of culturing cells at a liquid-liquid interface. He wanted to clarify the mechanisms that underlie cell-surface interactions, and believed that a) a liquid-liquid interface would be ideally suited to such studies, b) a liquid substrate would avoid the molecular inhomogeneities of a solid substrate, and c) proteins and phosphatide monolayers could be adsorbed to the interface to simulate half of a cell membrane. Rosenberg found that, for the most part, cells grew well on the liquid substrates he had chosen; however, their behavior was quite different on different oils. On FC-43 and FC-75, cells were not in contact with each other, and their growth was less sustained. On the other hand, cells were epithelial with uniform spreading on DC 710, 'Kel-F'-10 and 'Kel-F'-40 oils. He hypothesized that the differences were the results of variations in oil composition and impurities at the interface. He also studied the effects of different surfactants on cell growth. For example, cell spreading was reduced upon the injection of lecithin at the interface.

Cells grow on the layer of proteins adsorbed at the liquid-liquid interface. If proteins are not purposely pre-adsorbed, they are adsorbed from the culture medium. Due to the greater molecular homogeneity of liquids, the specific interactions of cells with a particular protein may be examined more directly than on a solid surface¹². Ando et al.¹² pretreated fluorocarbon-culture medium interfaces with extracellular matrix proteins (ECM) to determine their effects on cell attachment and growth. The density of human

endothelial cells was very low on untreated and bovine serum albumin (BSA)-treated interfaces, while it was significantly higher on interfaces treated with collagen type IV (COL), laminin (LN), fibronectin (FN), and fibrinogen (FG). Improving the strength of the adsorbed protein layer improves cell growth. Crosslinking the adsorbed protein layer with gluteraldehyde or inducing the formation of a double protein layer with polylysine lead to enhanced cell growth with reductions in the formation of aggregates and openings in the cell sheet⁷.

Different cell types behave differently at the liquid-liquid interface. Bovine endothelial cells grew on untreated interfaces, albeit with lower attachment and proliferation rates than for treated surfaces. Human endothelial cells, however, required treatment with ECM in order to show any growth¹². 3T3-L1 cells attached and spread to form a nearly confluent monolayer on the FC-70 interface, while SV-T2 cells formed aggregates⁷. Different cell types may exert different forces on the interface, causing the protein layer to break up and form aggregates^{12,13}. An alternative explanation may be that cells exert the same force but the surface area of their attachment plaques to the substrate varies. The force is delocalized for cells with larger plaques, leading to less damage and strain¹³. Greater attractive forces between cells may also lead to the formation of aggregates¹².

Surface-active compounds or surfactants, often present as trace impurities in fluorocarbons, facilitate cell growth at the liquid-liquid interface. Shiba et al.³ found little difference in cell growth and morphology among the fluorocarbons they studied, despite differences in their physical properties, leading them to conclude that cell growth may not

depend on the physical properties of the liquid-liquid interface. Two of the fluorocarbons studied by Keese and Giaever⁶, FC-72 and L-2345, exhibited very different cellular behavior even though they had very similar compositions. They attributed this difference to trace impurities in the compounds. Several studies have found that a fluorocarbon's ability to support cell growth is lost or decreased upon alumina column purification^{6,12,14}. Treatment of FC-43 with fibrinogen after purification showed decreased cell attachment and proliferation compared to unpurified, fibrinogen treated FC-43¹². While protein does adsorb at a purified interface, the interactions between the protein molecules are weaker and succumb more readily to forces exerted by cells⁶. Purified fluorocarbons regain their ability to support cell growth upon addition of surfactants. For example, addition of pentafluorobenzoyl chloride (F₅BzCl) to purified fluorocarbons restored the ability to support cell growth up to a concentration of 2 µg/ml⁶. Greater concentrations resulted in a loss of cell growth and spreading as a result of toxicity. Impurities containing hydrogen also restored cell growth¹⁴.

While growth is mainly dependent on surface-active impurities, the underlying liquid substrata have an effect on both growth and morphology. Sparrow et al.¹⁴ found differences in growth between different alumina treated fluorocarbons. The high stability of C-F bonds makes saturated perfluorocarbons practically inert while heteroatoms such as nitrogen and oxygen increase surface reactivity, leading to better cell growth even with alumina purification.

Cells do not adhere as strongly to a liquid substrate as to a solid substrate. The low degree of adhesiveness enhances the attractiveness of the liquid-liquid interface to certain studies, since strong adhesion is thought to interfere with rapid cell division. Shiba et al.³ noticed an accelerated growth rate for L-929 cells on a liquid substrate as opposed to a solid one, which they attributed to weaker cell adhesion to the liquid-liquid interface. Kwon et al.¹⁵ reported enhanced gene transduction on FC-40 interfaces treated with poly-L-lysine (PLL), gelatin (GN), and fixed gelatin (fGN) as opposed to polystyrene surfaces. They attributed this improved transduction to the flexibility of the FC-40 interface, also noting that the transduction efficiency was less for the fGN-treated FC-40, which exhibited the lowest transduction efficiency of the three protein-precoated interfaces before contact inhibition took place.

The low degree of adhesiveness lends itself to the study of membrane proteins produced by adherent cells. Cells can be removed without the use of trypsin-EDTA or scraping, both of which tend to damage the cell and alter the membrane proteins recovered. Terada et al.¹⁶ found that there was a difference in the amount of protein recovered between cells grown on plastic removed with either scraping or trypsin-EDTA and cells grown at a liquid-liquid interface and removed by pipetting. Trypsin-EDTA treatment had the most diminished protein recovery while scraping only differed a little from pipetting cells from the liquid interface. Sobel and Rosenberg¹⁷ reported similar findings. They noted that there was no evidence of cell damage when cells were pipetted from a liquid-liquid interface, as opposed to the harsher treatments of scraping or trypsinization used in studies of cell membrane proteins on a solid substrate.

Rappaport et al. reported multilayer growth for HeLa¹⁸ and Hep G2⁴ cells at the liquid-liquid interface. They found that multilayer growth depended on providing higher and more uniform oxygen concentrations to cells, a substratum with a lesser degree of adhesiveness, and a nutrient rich culture medium⁴. Perfluorocarbons have a high degree of O₂ solubility as well as being more flexible with a lower degree of adhesiveness. They determined that, in this environment, cells were able to produce albumin in greater quantities per cell than those growing on a solid substrate.

2.2 Total Internal Reflection Fluorescence

Total internal reflection fluorescence (TIRF) is a non-invasive technique used to study molecular interactions at interfaces. In TIRF, an evanescent wave is generated when a light beam, traveling in a medium of high refractive index, is totally internally reflected at the interface between the medium and one of a lower refractive index. The evanescent wave can be configured for shallow penetration (≤ 100 nm) into the medium of lower refractive index, which then selectively excites significantly more fluorophores at the interface than in the bulk. The fluorescence emission intensity curves provide information on the degree of molecular binding at the interface. For example, the concentration of a species can be determined as a function of distance from the interface, allowing the adsorption and desorption kinetic rates to be determined¹⁹.

TIRF has been used for a wide variety of studies, foremost among which are those that target biological phenomena. For example, TIRF has been used for visualization of cell-

substrate contact regions and the long term observation of cells, which is made possible because the short penetration depth of the evanescent wave limits damage to photosensitive cell organelles²⁰. TIRF may be used to measure kinetics of binding of proteins at interfaces, or to characterize receptor-ligand interactions. For example, in a recent study, Conboy et al.²¹ examined the interaction of HIV-1 surface glycoprotein gp 120 (rgp 120) with lactosylceramide (LacCer), glucosylceramide (GlcCer), and galactosylceramide (GalCer) in planar supported lipid bilayers. Binding to glycoproteins in the cell membrane is one of the first steps for HIV entry into a cell. They found that, at rgp 120 concentrations between 0.2 and 15 nM, rgp 120 has a high affinity for GalCer only.

The effect of surface properties on protein adsorption and desorption in the presence of other proteins are often studied with TIRF as well. Hlady and Ho²² studied the effect of human serum albumin (HSA) on the adsorption of low density lipoprotein (LDL) in relation to the hydrophobicity of the adsorbent surface. They reported that the kinetics of LDL adsorption and LDL apparent binding affinity decrease with increasing hydrophobicity. They found that the kinetics of LDL adsorption on hydrophilic silica was not affected by the co-adsorption of HSA, and pre-adsorption of HSA slowed the adsorption of LDL on silica with an even more significant decrease on the more hydrophobic end of the sample. TIRF spectroscopy has also been used for the detection of individual molecules at an interface^{20,23}.

The total internal reflection geometry can be combined with a variety of other spectroscopic techniques. When combined with fluorescence photobleaching recovery (FPR), the kinetics of desorption of molecules from an interface can be determined^{24,25}. Similarly, TIR can be combined with fluorescence correlation spectroscopy (FCS), which monitors the random fluctuations in the number of fluorophores in a very small observation volume, to determine the kinetic rate and bulk diffusion near the surface²⁴. TIR and resonance light scattering (RLS) have also been used to characterize interfacial species without the use of fluorescent dyes, while limiting interference from other molecules that is commonly observed in bulk solutions²⁶. TIR-fluorescence lifetime measurements provide information on the molecular state and structure of fluorophores at an interface²⁰.

Various studies using total internal reflection have been performed at the liquid-liquid interface. Gajraj and Ofoli²⁷ developed a total internal reflection fluorescence microscopy (TIRFM) apparatus to examine the liquid-liquid interface, using a geometry in which the entire oil-water layer was about 1.0 mm thick. They studied the adsorption of bovine serum albumin (BSA) and lysozyme at the interface, to determine if the thin oil-water interface was thermodynamically true. They were able to accurately estimate the critical micelle concentration of BSA, demonstrating that the thin oil-water layer accurately mimics a standard interface. The adsorption dynamics of a protein to a liquid-liquid interface can be affected by conditions at the interface, as well as conditions of the molecule itself. Using the same apparatus, Gajraj and Ofoli²⁸ examined the effects of fluorescent labels on the adsorption kinetics and diffusion of BSA at the oil-water

interface using TIR/FPR. They reported that the apparent diffusion coefficient of BSA labeled with two FITC (BSA-2FITC) molecules was about 40% greater than that of BSA labeled with only one FITC molecule. BSA-2FITC also had a slower rate of desorption from the interface. These differences were attributed to increased hydrophobicity with increased labeling ratio.

Jones and Bohn^{29,30} used TIRF in conjunction with electrocapillary measurements to monitor the potential dependent adsorption of dye di-Nbutylaminonaphthylethenylpyridiniumpropylsulfonate (dye I), a zwitterionic amphiphile, at bare and dilauroylphosphatidylcholine (DLPC)-modified 1,2-dichloroethane (DCE) -water interfaces. The fluorescence behavior of dye I changed in the presence of DLPC. Without DLPC, the probe fluorescence decreased with increasingly positive potentials over 0.25 V but, with it, fluorescence emission increased with increasingly positive potentials over 0.29 V. This behavior was attributed to the formation of dye I aggregates, which do not fluoresce, on the bare interface. On the other hand, the surface excess of dye I was reduced and aggregates could not be readily formed on the DLPC modified interface. This was because, as more dye I replaced DLPC, the affinity for the interface drops with increasingly positive potential.

Hashimoto et al.²³ developed a method to detect single molecules adsorbed at the dodecane-water interface. The lateral diffusion coefficient of single cyanine dye molecules (DiI) was estimated from the maximum duration of photon bundles detected in the observation area. The effects of two surfactants, sodium dodecyl sulfate (SDS) and

dimyristoyl phosphatidylcholine (DMPC), on the lateral diffusion dynamics of DiI were also investigated. The lateral diffusivity of DiI was only slightly affected by the presence of SDS, while DMPC drastically reduced it.

The physical properties of the liquid-liquid interface can also be examined with TIRF. Ishizaka et al.³¹ studied the polarity of several oil-water interfaces with sulforhodamine B (SRB), a polarity sensitive probe. The roughness/thickness of the oil-water interface was determined by fluorescence dynamic anisotropy and excitation energy transfer dynamics and related to the interfacial polarity determined by TIRF spectroscopy. For thin, sharp oil-water interfaces, the interfacial polarity was well predicted by the arithmetic average of the polarities of the water and oil phases. Cyclohexane-water, CCl₄-water, and toluene-water interfaces were considered thin and sharp. On the other hand, when the oil-water interface was determined to be rough, the interfacial polarity deviated from the average as in the case of dichlorobenzene-water and DCE-water interfaces. Oils with higher polarity tended to form rough interfaces. Hashimoto et al.²³ estimated the interfacial viscosity, η_i , from the lateral diffusion dynamics determined by single molecule fluorescence at the dodecane-water interface. The interfacial viscosity was as high as that for dodecane (1.4 mPa s) and higher than the value for water (0.89 mPa s). In the presence of SDS, the interfacial viscosity was slightly higher than that of dodecane. In the presence of DMPC it was two orders of magnitude greater.

Yamashita et al.³² used time-resolved TIRF spectroscopy to study the solvation dynamics of 12-(9-anthroyloxy) steric acid (12-AS) and 4-(9-anthroyloxy) butanoic acid (4-ABA) at

the heptane-water interface. These probes are sensitive to changes in their solvated environments due to strong charge-transfer in the excited state. 12-AS is soluble in heptane while 4-ABA is water-soluble. From observation of the time-dependent fluorescence spectral shifts, it was determined that 4-ABA was surrounded by more water molecules and was located closer to the water phase than 12-AS. The solvent relaxation of 12-AS occurred more slowly at the interface than in the bulk solution.

Feng et al. used TIRF at the CCl_4 -water interface to determine the amounts of chlortetracycline (CTC)³³ and berberine³⁴, and TIR/RLS to determine the amount of HSA³⁵ present in a sample. CTC is an antibiotic drug often used in medicine and food science. Berberine is used to cure digestive system ailments. In the case of CTC, a fluorescent complex was formed between CTC, europium (III), and trioctylphosphine (TOPO) at the CCl_4 -water interface. TOPO was dissolved in the CCl_4 phase while CTC and Eu(III) were dissolved in the water phase. The fluorescence of berberine was enhanced when it was adsorbed at the CCl_4 -water interface in the presence of sodium dodecyl benzene sulfonate (SDBS). A complex that was formed between HSA, thorium (IV), and SDBS resulted in enhanced TIR/RLS signals at the CCl_4 -water interface. To determine the sensitivity and selectivity of the TIRF or TIR/RLS signal, model samples were made by adding other substances such as metal ions, amino acids, and carbohydrates. γ -globulin was added to model solutions for HSA as it interferes with most common HSA assays. Body fluid samples were also used to detect CTC and HSA. The TIRF and TIR/RLS detection methods were accurate in all three cases and there was limited interference from the other substances. There was no interference from γ -globulin

in the case of HSA. The TIR assay methods were simpler and less time consuming than many of the assays currently in use for the quantification of these compounds in a sample.

3. THEORETICAL CONSIDERATIONS

3.1 Total Internal Reflection

The theory of total internal reflection is well developed elsewhere¹⁹. Briefly, a light beam traveling from an optically dense medium, with refractive index n_1 , to an optically rarer medium, with refractive index n_2 , will be totally internally reflected when the angle of incidence, measured from the normal to the interface, exceeds a critical angle, θ_c , where

$$\theta_c = \sin^{-1}\left(\frac{n_2}{n_1}\right). \quad (3.1)$$

Although the beam is totally internally reflected at the interface, it produces an electromagnetic field called the evanescent wave, which penetrates into the rarer medium (Figure 3.1). The intensity of the evanescent wave, $I(z)$, decays exponentially with distance, z , from the interface according to the relationship

$$I(z) = I(0) \exp\left(-\frac{z}{d}\right) \quad (3.2)$$

where $I(0)$ is the intensity of the incident light at the interface and d , the penetration depth, is given by

$$d = \frac{\lambda_0}{4\pi\sqrt{n_1^2 \sin^2 \theta - n_2^2}}. \quad (3.3)$$

λ_0 is the wavelength of incident light at the interface. The penetration depth, d , is independent of the polarization of the light beam. It is on the order of λ_0 or less and decreases with increasing θ , except as $\theta \rightarrow \theta_c$, in which case $d \rightarrow \infty$.

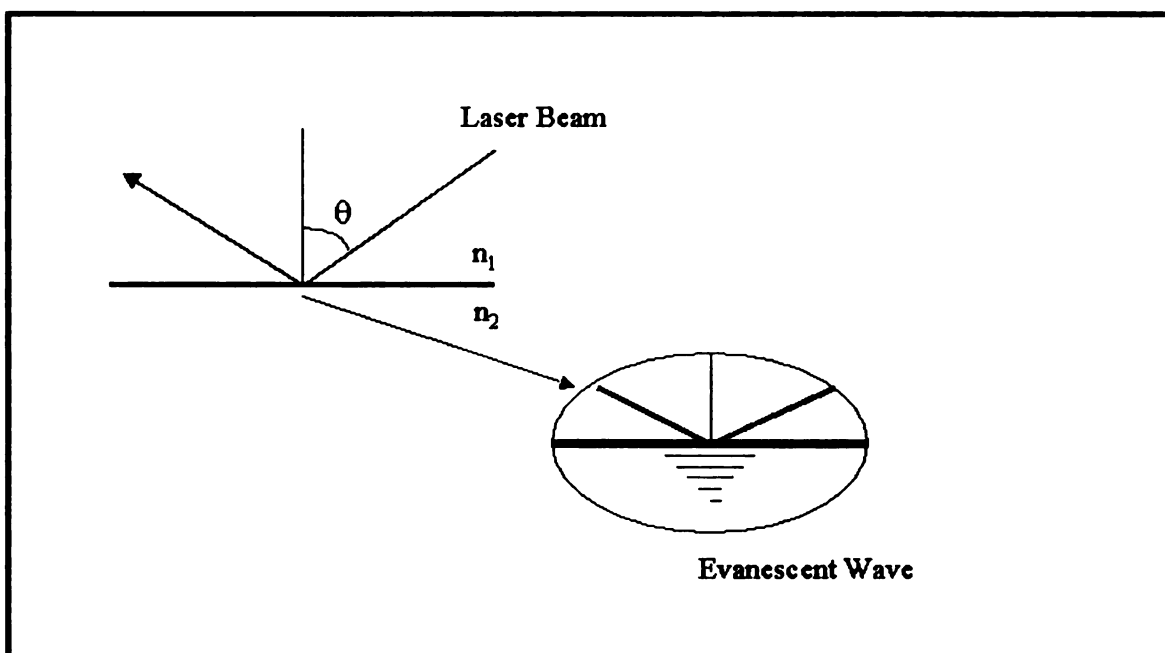
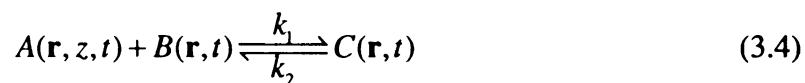


Figure 3.1: Total internal reflection at an interface, induced by laser beam entering the interface at an angle exceeding the critical angle. The resulting evanescent wave decays exponentially with distance into the optically rarer medium.

3.2 Fluorescence Photobleaching Recovery

The theory of total internal reflection/fluorescence photobleaching recovery (TIR/FPR) is well treated elsewhere^{24,25}. In its essence, the binding of molecules to the interface may be represented by the chemical equation:



where $A(\mathbf{r}, z, t)$ is the bulk concentration of molecules, $B(\mathbf{r}, t)$ is the surface concentration of free binding sites, and $C(\mathbf{r}, t)$ is the surface concentration of bound molecules. The constants k_1 and k_2 are the surface adsorption and desorption rate constants respectively. The equilibrium constant, K , is then

$$K = \frac{[C]}{[A][B]} = \frac{k_1}{k_2}, \quad (3.5)$$

where $[A]$, $[B]$, and $[C]$ are the equilibrium concentrations.

Assuming that molecules within the evanescent wave are bound to the surface, the measured fluorescence, $F(t)$, is then

$$F(t) = QI_0 \int \mathcal{I}(\mathbf{r}) C(\mathbf{r}, t) d^2\mathbf{r}, \quad (3.6)$$

where Q is a product of the efficiencies of excitation light absorption and fluorescence emission and detection, I_0 is the maximum intensity and $\mathcal{I}(\mathbf{r})$ is a dimensionless profile function with a maximum amplitude of unity.

For FPR

$$G(t) = \bar{F} - F(t) \quad (3.7)$$

where $F(t)$ is the fluorescence emission after photobleaching at time $t = 0$ and \bar{F} is the equilibrium pre-bleach fluorescence emission intensity. The surface concentration of unbleached fluorescent molecules, $\mathcal{C}(\mathbf{r}, t)$, is

$$\mathcal{C}(\mathbf{r}, t) = [C] - C(\mathbf{r}, t) \quad (3.8)$$

Combining Equations (3.6), (3.7) and (3.8), we obtain

$$G(t) = QI_0 \int \mathcal{I}(\mathbf{r}) \mathcal{C}(\mathbf{r}, t) d^2\mathbf{r} \quad (3.9)$$

To solve for $G(t)$, the differential flux equations for $A(\mathbf{r}, z, t)$ and $C(\mathbf{r}, t)$ are solved by linear transformation theory, with initial conditions derived from the intensity profile of

the monitoring beam and boundary conditions based on the fact that only surface bound molecules within a finite surface area are bleached.

After integration and application of the boundary conditions, $G(t)$ can be simplified based on the conditions of the system. The simplest form of $G(t)$, and the one for which the theory is best defined, is that of the “reaction limited” regime, where bulk diffusion is rapid relative to the adsorption and desorption of molecules from the interface. In this case

$$G(t) \approx G(0) \exp(-k_2 t). \quad (3.10)$$

To determine if the system is in the reaction limited regime, the characteristic time for bulk diffusion, $(1/R_{BND})$, is calculated

$$\frac{1}{R_{BND}} = \frac{([C]/[A])^2}{D_A} \quad (3.11)$$

where D_A is the bulk diffusion coefficient. If the characteristic time of recovery in a TIR/FPR experiment is much larger than $1/R_{BND}$, then the experiment is reaction limited.

Once it is determined that the experiment is reaction limited, the fluorescence recovery curve, $F(t)$, is normalized to give $g(t)$:

$$g(t) = 1 - \frac{F(t) - F(0)}{\bar{F} - F(0)} \quad (3.12)$$

where \bar{F} is the equilibrium pre-bleach fluorescence intensity, $F(0)$ is the intensity immediately following photobleaching at time $t = 0$, and $F(t)$ is the subsequent

fluorescence recovery. The variable $g(t)$ is $G(t)/G(0)$ as defined by Equation (3.7), and can be written as the sum of exponentials:

$$g(t) = g_0 + \sum_{i=1}^m g_i \exp(-k_2(i)t) \quad (3.13)$$

where g_0 is the fraction of molecules which are irreversibly bound to the interface, the g_i are different binding classes of molecules (for example, rapidly versus slowly desorbing), and the $k_2(i)$ are the desorption rates of those classes. The parameters are determined by curve fitting.

4. EXPERIMENTAL MATERIALS AND TECHNIQUES

4.1 Materials

Fluorinert liquid FC-70 was purchased from 3M (St. Paul, MN). FC-70 was sonicated for 30 minutes to improve stability at the interface⁴ and sterilized by exposure to UV-light for up to 24 hours and/or by passage through a 0.22- μ m filter (Millipore Corporation, Bedford, MA). Human plasma fibronectin (FN) (FC010, Chemicon International, Temecula, CA) and human serum albumin (HSA) (A8763, Sigma Chemical Co., St. Louis, MO) were dissolved in PBS buffer solutions (pH 7.4) to give the concentrations required for each experiment. Both protein solutions were sterilized by passage through a 0.22- μ m filter. Fluorescein-5-isothiocyanate (FITC) was purchased from Molecular Probes (F1907, Eugene, OR).

NIH/3T3 (ATCC) fibroblasts were generously provided by Dr. C. Chan, Michigan State University. Culturing was done in a humid 37°C, 5% CO₂ incubator (Class II Water Jacketed CO₂ Incubator, Thermo Forma, Marlotta, OH) in a pH 7.4 culture medium consisting of Dulbecco's Modified Eagle's Medium (DMEM) (GIBCO, Carlsbad, CA) supplemented with 10% fetal bovine serum (GIBCO, Carlsbad, CA). Industrial grade CO₂ was purchased from AGA Gases (Lansing, MI) at a purity of 99%.

4.2 Experimental Methods

4.2.1 Cell Culture

4.2.1.1 Preparation of liquid-liquid interface for cell culture

The liquid-liquid interface was prepared following the method of Ando et al.¹². In a sterile biological safety cabinet (Class II A/B3 Biological Safety Cabinet, Thermo Forma, Marlotta, OH) FC-70 was added to the wells of a 48-well tissue culture plate (Corning Incorporated, Corning, NY) to give oil layer thicknesses of 5 mm, 1 mm, and 0.5 mm. After this, 0.7 ml of either 4 µg/ml FN solution or 1 mg/ml HSA solution was carefully pipetted on top of the oil. The plate was then incubated at 37°C for approximately three hours. After incubation, the protein solution was removed and the interfaces gently washed three times with culture medium. After that, 0.5 ml of cell suspension was pipetted on top of the interface.

4.2.1.2 Growth Curves

Growth curve experiments were run over a period of up to four days for each of the oil layer thicknesses and at least one of two controls: an untreated 5 mm thick fluorocarbon layer, and plastic. Cells were removed from the interface with trypsin-EDTA (GIBCO, Carlsbad, CA) and scraping and counted using a hemocytometer. Duplicates of each sample were counted.

4.2.2 TIRFM/FPR

4.2.2.1 TIRFM Apparatus

The experimental setup (Figure 4.1) is described in detail elsewhere²⁷. The system uses an inverted microscope (Zeiss Axiovert 135 M, Carl Zeiss, Inc., Thornwood, NY), which houses a motorized stage and flow cell. The 488 nm line of a 5W continuous wave argon ion laser (Lexel Lasers Model 95, Fremont, CA) was used in all experiments. Intensity measurements were made with a side-on photomultiplier tube (PMT) (Hamamatsu R4632, Bridgewater, NJ) jacketed in a thermoelectrically cooled housing (TE177TSRF, Products for Research, Danvers, MA). A modular automation controller with an RS232 interface (MAC 2000, Ludl Electronic Products, Hawthorne, NY) provides the high voltage required for PMT operation. A double-syringe pump system (Model 551382, Harvard Apparatus, South Natick, MA) simultaneously infuses and withdraws samples from the flow cell, to prevent damage to the interface. The entire apparatus, with the exception of the automation controller, is mounted on a vibration isolation table (RS 4000, Newport Corporation, Irvine, CA) to ensure interfacial stability.

The laser beam is attenuated using neutral density filters (03FNQ, Melles Griot, Boulder, CO). An optical chopper (SR540, Stanford Research Systems, Sunnyvale, CA) prevents unintended photobleaching when long experiments are being conducted. A system of two optical flats and a programmable shutter (D122, Uniblitz, Vincent Associates, Rochester, NY) are used to split the laser beam into a photobleaching and a much weaker monitoring beam such that the ratio of the two intensities is approximately 10,000:1. The first flat

splits the beam while the second flat recombines the two so that they are accurately superimposed at the interface. Between the two flats, the shutter blocks only the photobleaching beam. When activated, the shutter allows for photobleaching with a sub-millisecond laser flash. After passing through the flats, the laser beam is conveyed by mirrors and finally focused onto the interface using a plano-convex lens ($f = 200 \text{ nm}$, Oriol Corporation, Stratford, CT).

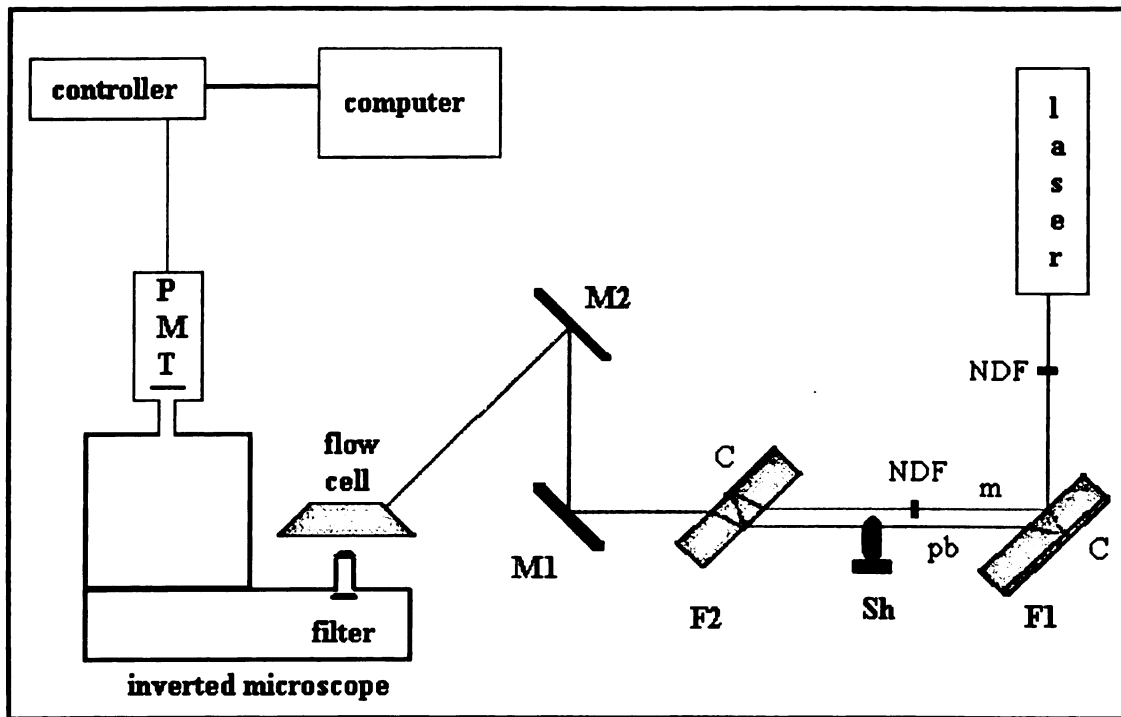


Figure 4.1: The experimental set up for TIRFM. The double flat system (F) splits the beam into an intense photobleaching beam (pb) and a much weaker monitoring beam (m), and then recombines them to ensure that both beams are incident at the same spot on the interface. Mirrors (M) enable focusing of the beam into the sample cell²⁷.

A Zeiss LD achroplan microscope objective (440651, 32x, 0.4, Carl Zeiss Inc., Thornwood, NY) is focused at the interface and captures the fluorescence emission from the sample. An interference filter (500EFLP-EM, Omega Optical, Brattleboro, VT) inside the microscope allows the fluorescence emission wavelengths to be separated from the excitation wavelength. The PMT is operated in digital (photon counting) mode. A fast preamplifier (SR 445, Stanford Research Systems, Sunnyvale, CA) amplifies the output signal from the PMT, which is then fed to a photon counter (SR 400, Stanford Research Systems, Sunnyvale, CA) for measurements. Fluorescence intensities are recorded with programs written in Labview 6.0 (National Instruments, Austin, TX). An output reference voltage from the chopper triggers the photon counter so that data collection only occurs when the laser beam illuminates the sample cell.

The flow cell consists of two microscope slides separated by a 800 μm thin aluminum spacer with an oval cut into it to form the sample cell (Figure 4.2). The underside of the top slide is coated with Cargille immersion oil ($n = 1.46$, Fisher Scientific, Pittsburgh, PA). Oil layer thickness, ranging from 4 μm to 50 μm , was controlled by spin coating microscope slides with oil at different speeds. Higher speeds produced thinner oil layers. Two holes are cut into the bottom slide to allow for infusion and withdrawal of protein solutions by the double-syringe pump. The top slide is optically coupled to a 70° dovetail prism ($n = 1.46$) and the entire assembly is secured onto an anodized aluminum shell that sits on top of the microscope stage. The entire oil-water assembly for TIRFM experiments was approximately 800 μm thick.

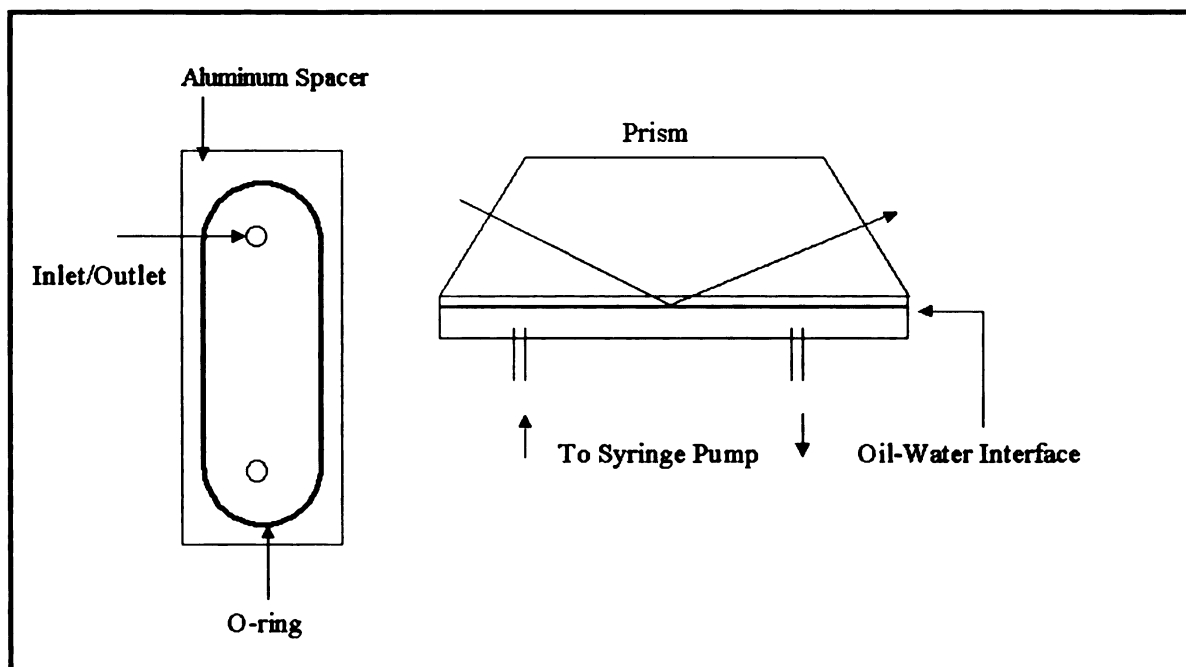


Figure 4.2: The experimental flow cell. Spin coating controls the thickness of the oil layer on the top slide. The entire oil-water assembly is approximately 800 μm thick.

4.2.2.2 Procedure for Labeling Proteins

Proteins were labeled following the procedure provided in the Molecular Probes product information for amine reactive probes³⁶. Approximately 10 mg of protein was dissolved in 5 ml of sodium bicarbonate buffer (0.1 M, pH 9.0). A labeling ratio of 1.3:1 was used to determine the appropriate concentration of FITC, dissolved in sodium bicarbonate buffer. The FITC solution was slowly added drop wise (about 50 μl) to the continuously stirred protein solution. The reaction was incubated at room temperature for 4 to 6 hours with continuous stirring. The stop reaction was performed using 0.1 ml of a 1.5 M hydroxylamine solution (pH 8.5) and incubated for an hour. Hydroxylamine removes dye from unstable conjugates with tyrosine, serine, threonine, and histidine³⁶. A dialysis process, performed over a period of 48 hours, was used to remove the unreacted dye. The

final protein concentration and labeling ratio were determined by measuring absorbance at 280 nm and 496 nm with a diode array spectrophotometer (8452 A, Hewlett Packard, Brielle, NJ).

4.2.2.3 Beam Alignment and Microscope Focusing Procedure

For the TIRFM system to be properly aligned, normal incidence of the laser beam on the prism must be achieved while the point of total internal reflection (TIR) is exactly above the microscope objective. First, the flow cell was filled with PBS buffer using the syringe pump. Normal incidence was accomplished by adjusting the mirrors until the back reflection from the prism is aligned along the original path of the laser beam. This indicated that normal incidence had been achieved. The position of TIR in the flow cell was then checked. If it was not over the microscope objective, the mirrors were adjusted in the opposite direction and the procedure for normal incidence was repeated.

To focus the microscope, the plano-convex lens was put into place and alignment was first done by eye to place the point of TIR over the objective. The interference filter was removed from the microscope. Then, looking through the PMT cavity on the microscope, the lens was adjusted to position the evanescent wave over the microscope objective. The microscope was then focused until the evanescent wave filled the objective. The shutter was then used to block the photobleaching beam, and the PMT was put into place on the microscope. Small adjustments were made to the microscope to maximize the PMT signal. The interference filter was then replaced in the microscope and the protein solution was injected into the flow cell.

4.2.2.4 Photobleaching

The flow cell was filled with protein solution for an hour, during which time readings were taken every 2 to 5 minutes until pseudo-equilibrium adsorption has been achieved. At this point, the chopper was switched off, the shutter was triggered, and the sample was subjected to a brief flash of the photobleaching beam for approximately 100 ms. During the photobleaching flash, a shutter in the microscope, which is triggered along with the other shutter, protects the PMT. After the photobleaching pulse, the fluorescence recovery was recorded.

4.2.2.5 Data Analysis

The data were analyzed with a user defined regression equation in Sigma Plot 2001 (SPSS Inc., Chicago, IL). An iterative method was used to determine the values of the coefficients in Equation (3.13). The regression program was provided with initial guesses of the coefficients; the resulting numbers were then input into the program as new initial guesses until the percent variance was minimized. An example of the output is given in Appendix B.

5. RESULTS AND DISCUSSION

5.1 Cell Culture

The attachment and growth of 3T3 fibroblasts at the interface between culture medium and FC-70 layers of 5 mm, 1 mm, and 0.5 mm was studied, with 0.5 mm being the minimum thickness attainable in our system. When a smaller layer of FC-70 was placed in the well, it completely covered the bottom of the well but, upon addition of culture medium, it would pool to the side of the well. Two other fluorocarbons, HFE-7100 and HFE-7500, were also investigated. These are primarily composed of hydrofluoroethers, and both exhibited the same tendencies observed with FC-70. The polystyrene culture plates used in this study were treated to make them hydrophilic and negatively charged, in order to promote cell attachment. The interaction between the hydrophobic fluorocarbons and the hydrophilic polystyrene plate is likely one of high energy. It is possible that, by pushing the medium off the interface so that the medium can directly interact with the plate is a mechanism to lower the total free energy of the system.

Results show that cell growth was influenced by the thickness of the FC-70 layer, most likely the result of better initial cell adhesion to the adsorbed protein layer. Figure 5.1 shows the growth curves (cell count versus time) for interfaces on which fibronectin (FN) had been adsorbed, and for one interface that was not pretreated with the protein. All cell counts data were normalized against the initial seeding density. Clearly, both growth and proliferation improved as the fluorocarbon layers became thinner. As was discussed in Chapter 1, this is most likely because thinner fluorocarbon layers promote interfacial stability of the adsorbed protein layer, which reduces protein layer rupture and subsequent

formation of lake-like openings in the protein film. The stronger protein film enables better cell attachment, growth and proliferation.

The cell morphology is shown in Figure 5.2 for the 0.5 mm and 1 mm layer thicknesses. The cell sheets were nearly confluent in both cases, with slightly bigger openings in the 1 mm case. The cells were more densely packed on the 0.5 mm thick fluorocarbon layer, even though there are still some areas in the sheet with only a sparse covering of cells. The cells on the 1 mm thick layer have densely packed areas, but there are larger cell-free gaps. The cells appear to be forming an aggregate (see the dark spot in Figure 5.2 B), which is probably the result of breakage of the protein monolayer as the cells grow and proliferate. Phase contrast images could not be taken of the 5 mm thick layer on the available microscope because it could not be precisely focused on the interface. Cell growth on the 5 mm interface was observed on another microscope in the lab, to ensure that the growth was as expected.

Cell growth and proliferation studies were also conducted with human serum albumin (HSA) adsorbed at the liquid-liquid interface, to provide a comparison for the data obtained for FN. Results were similar to those for FN with regards to the effect of fluorocarbon layer thickness. Figure 5.3 presents the growth curves for HSA. The cell morphology on 1 mm and 0.5 mm HSA-treated FC-70 layers is shown in Figure 5.4. There are large cell-free gaps on the HSA-treated FC-70-media interfaces, and aggregates appear to be forming on the 1 mm thick fluorocarbon layer. In comparison to FN, cells did not grow as well on adsorbed HSA, and the cell sheets were not as confluent.

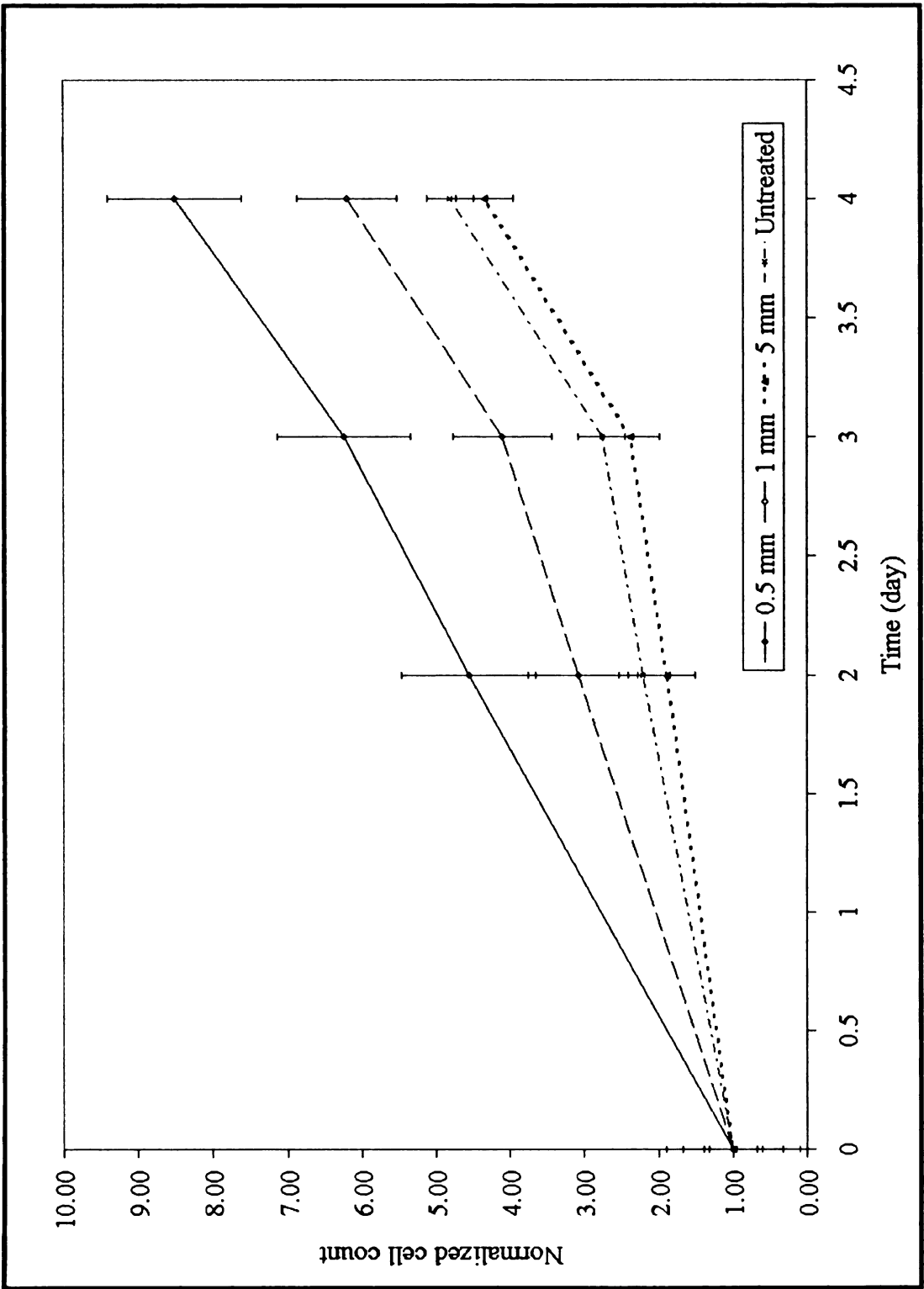


Figure 5.1: Growth curves for FN-treated FC-70-culture media interfaces. 'Untreated' refers to a 5 mm FC-70 layer on which FN was not adsorbed prior to the cell culture experiment. Lines do not represent models, but have been added to aid in visualizing trends. All cell count data were normalized against the initial seeding density.

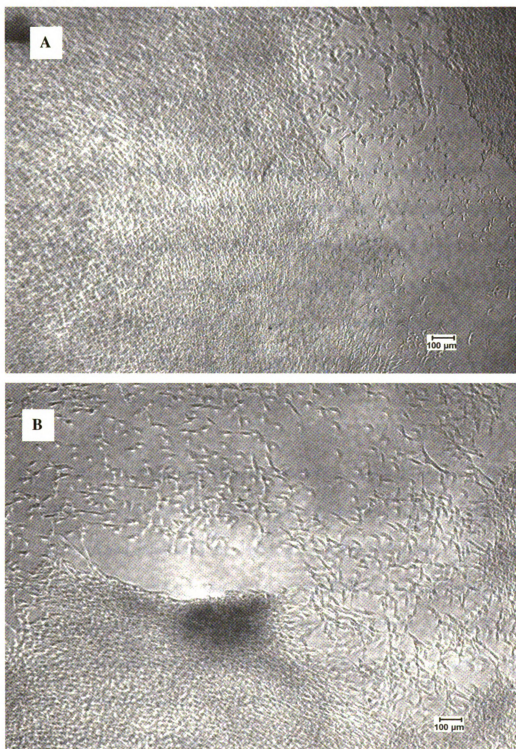


Figure 5.2: Cell behavior on 0.5 mm (A) and 1 mm (B) FN-treated FC-70 layers, after 3 days of incubation. There are only a few small cell-free gaps on the 0.5 mm layer (A). However, there is evidence of more protein layer rupture and aggregate formation (dark spot) on the 1 mm layer (B). The two images are of identical magnification.

Figure 5.5 shows the cell counts as a function of FC-70 layer thickness for adsorbed HSA and FN, for 2, 3, and 4 days. For the entire culture period, growth was better on the 0.5 mm and 1 mm FN-treated interfaces than those treated with HSA. In the 5 mm case, the only major difference in cell numbers was on the final day of culture, where the FN-treated interface had more cells. Cell layers were more densely packed on FN-treated interfaces than on those treated with HSA (Figure 5.6). In comparison to FN, there are large areas on the HSA-treated interface where cells have not grown at all. In light of data recently acquired in our laboratory³⁷, it would be expected that FN-treated interfaces would promote greater initial cell attachment and subsequent growth than those treated with HSA, since FN adsorbs more strongly at the interface than HSA. Therefore, the trend observed in this study is as expected.

As a control, experiments were also conducted on an untreated surface with a 5 mm layer of FC-70. As can be seen in Figures 5.1 and 5.3, there was not much difference between protein-treated and untreated 5 mm layers with respect to the density of cells growing on them. The probable reason is that, at this FC-70 layer thickness, the interactions between the adsorbed proteins and the underlying substrate are not as strong as they are in the cases where the interface is much closer to the underlying solid. Therefore, the cells can tear the protein monolayer apart as they proliferate and move around on the surface, leading to reduced cell growth.

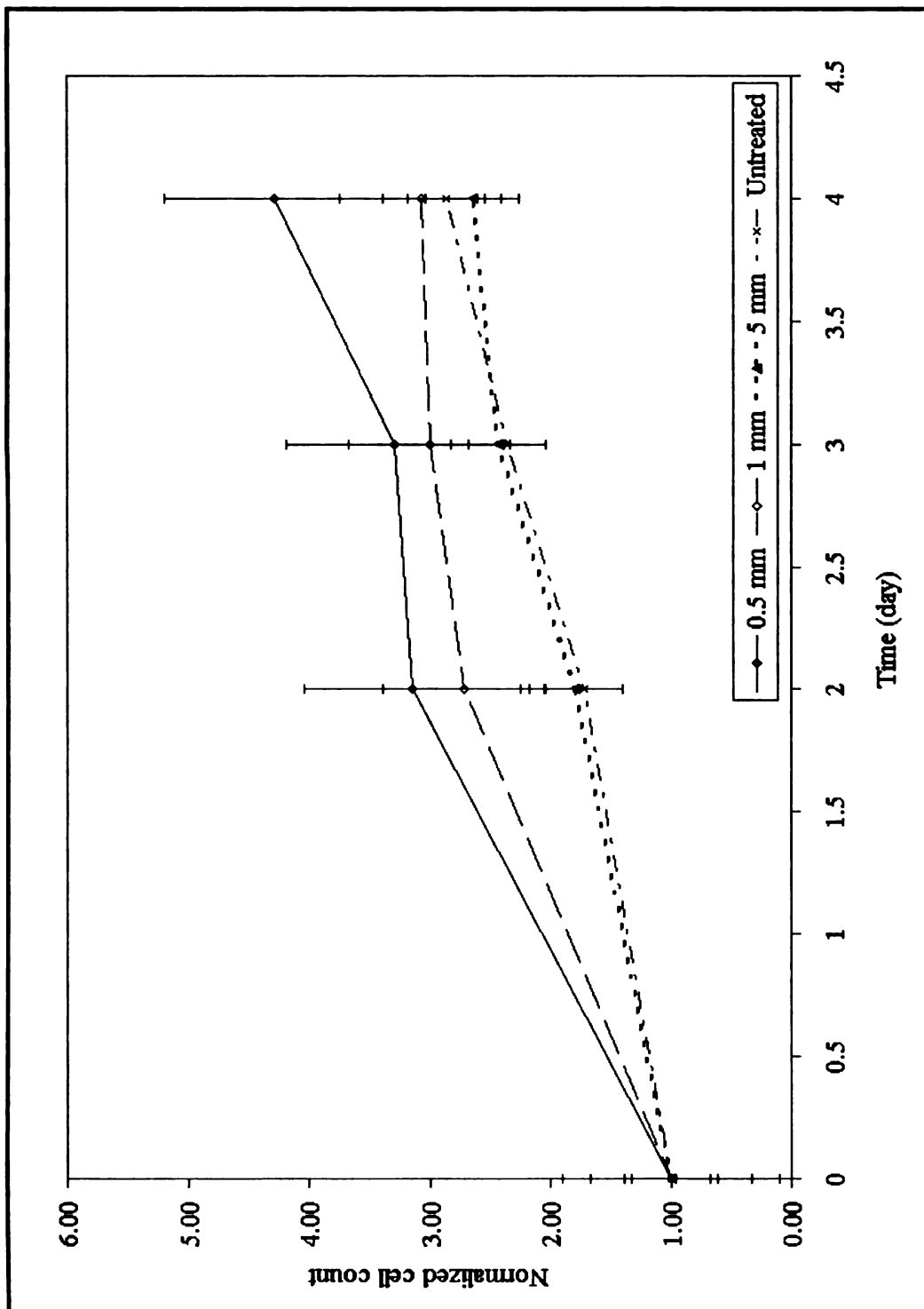


Figure 5.3: Growth curves for HSA-culture media interfaces. 'Untreated' refers to a 5 mm thick FC-70 layer on which HSA was not adsorbed prior to the cell culture experiment. Lines have been added to aid in visualizing trends. All cell count data were normalized against the initial seeding density.

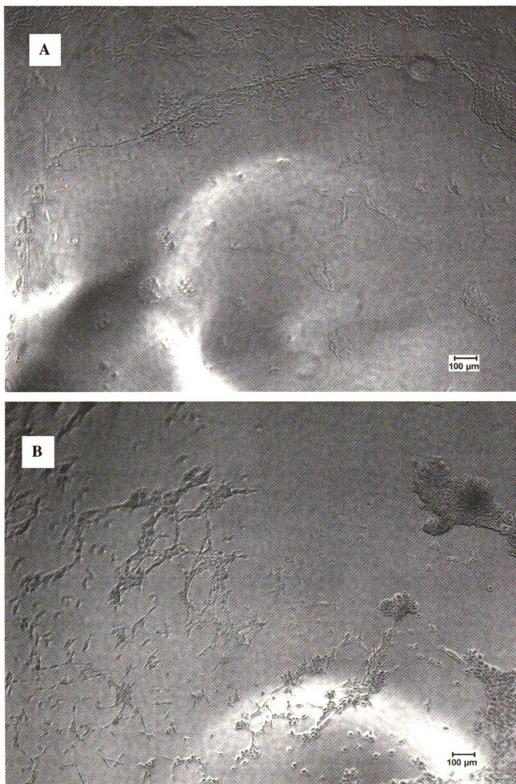


Figure 5.4: Cell behavior on 0.5 mm (A) and 1 mm (B) HSA-treated FC-70 layers, after 3 days of incubation. Cell growth in both cases is sparse. There are more and larger aggregates (dark spots) on the 1 mm layer (B).

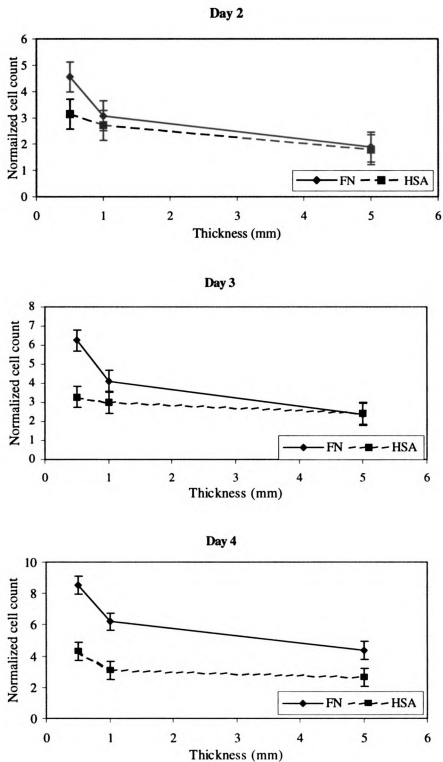


Figure 5.5: Cell count as a function of fluorocarbon layer thickness for FN and HSA on Days 2 (top), 3 (middle), and 4 (bottom). Lines have been added to aid in visualizing trends. All cell count data were normalized against the initial seeding density.



Figure 5.6: Cell growth on 0.5 mm FC-70-culture media interfaces after 3 days of incubation for FN (A) and HSA (B). Cell growth on the FN-treated interface is clearly much more robust than on the HSA-treated interface.

It is reasonable to expect that cells could be more easily removed from the liquid-liquid interface than from the solid-liquid interface. As a result, it was originally hypothesized that trypsin-EDTA treatment would be enough to ensure that all the cells were removed from the liquid-liquid interfaces. However, it turned out that trypsin-EDTA treatment alone was not enough to remove cells, especially in the case of FN. Figures 5.7, 5.8, and 5.9 show images before and after trypsin-EDTA treatment for FN, HSA, and bare plastic, respectively. Cells are generally ready for removal when they have detached from the interface and “rounded up”¹. In the cases of plastic and HSA, the cells had rounded up and were ready to be pipetted off. For FN, however, there were still quite a few cells that had not rounded up even after 20 minutes of treatment with trypsin-EDTA. A possible explanation for this is that serum proteins, such as fibrinogen in the culture medium, interact with FN adsorbed at the liquid-liquid interface, thus strengthening cellular adhesion⁸. It is likely that FN is interacting with the cells as well as the interface; this may be over-riding the normal route of detaching cells with trypsin-EDTA.

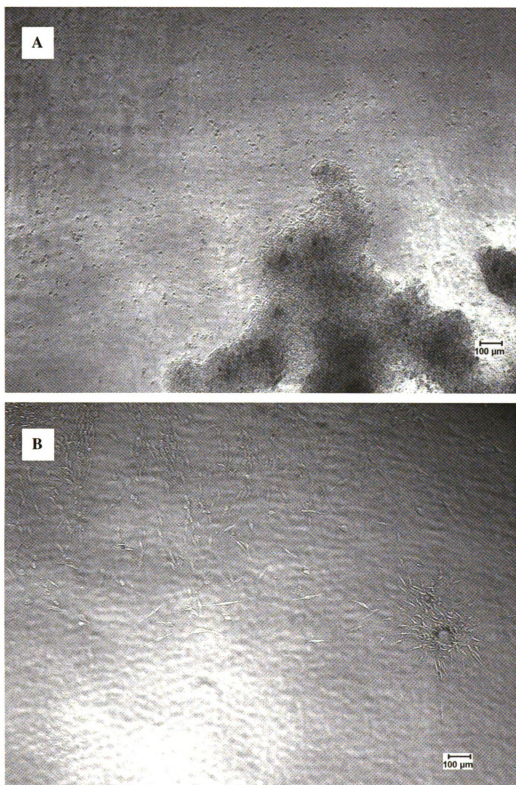


Figure 5.7: Cells before (A) and after (B) 20 minutes of trypsin-EDTA treatment on 1 mm of FN-treated FC-70-medium interface. The cells have not rounded up after being treated with trypsin-EDTA, so they cannot be completely removed by trypsin-EDTA treatment.

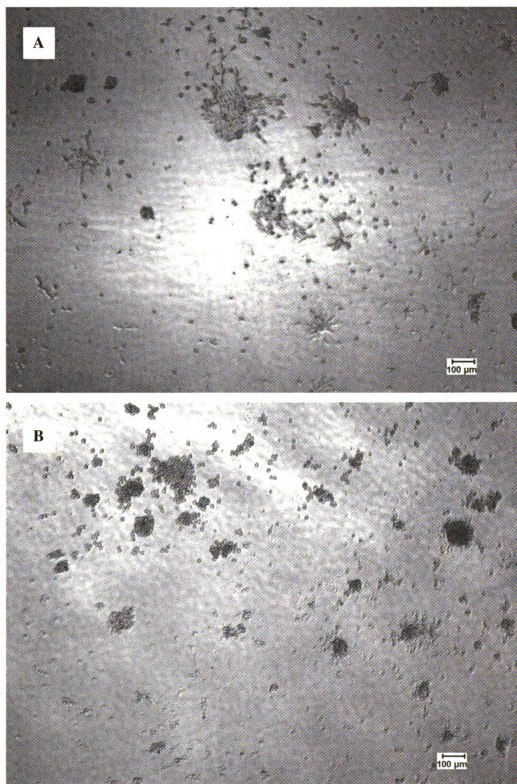


Figure 5.8: Cells before (A) and after (B) 20 minutes of trypsin-EDTA treatment on 1 mm of HSA-treated FC-70-medium interface. Most of the cells have rounded up and are ready to be detached after trypsin-EDTA treatment.

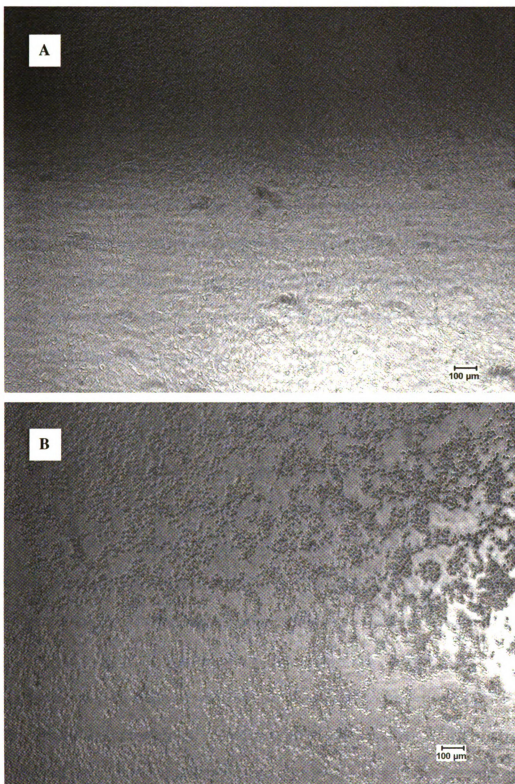


Figure 5.9: Cells before (A) and after (B) 20 minutes of trypsin-EDTA treatment on polystyrene culture plate. All of the cells have rounded up and are ready to be removed from the plastic surface (B).

5.2 TIRFM/FPR

The adsorption of protein was studied at the liquid-liquid interface with TIRFM/FPR at oil-water interfaces featuring oil layers ranging in thickness from 4 μm to 50 μm . A typical fluorescence recovery curve for HSA is shown in Figure 5.10. After equilibrium adsorption, the interface was exposed a brief flash of the bleaching beam. The subsequent fluorescence emission intensity is approximately 60% of its pre-bleach level. The recovery is slow, indicating a slow exchange of interface-bound bleached proteins with unbleached protein from the bulk. This implies that a large fraction of protein is irreversibly bound to the interface.

The gaps in the curve result from the fact that, to prevent photobleaching over the long duration of the experiment, the monitoring beam was periodically blocked for a few seconds as the data were acquired. The fluorescence recovery data from Figure 5.10 were normalized with Equation (3.12) and then fitted to Equation (3.13), using Sigma Plot. Data were fitted with $i = 1$ (see Eqn. (3.13)). The purpose of the second exponential term in the equation was to help model the kinetics of recovery of the slowly desorbing class of molecules. However, the timescale over which the recovery data were collected (approximately 95 seconds) was most likely too short to see the dynamics of the slowly desorbing class of molecules. As a result, the double exponential form of the equation ($i = 2$) was not used to fit the experimental data. However, since the irreversibly adsorbed, rapidly desorbing and slowly desorbing fractions must add up to unity, the slowly

desorbing fraction can be determined from the single exponential fit, even though the kinetic rate of that fraction is not captured by this procedure.

Sample $g(t)$ data are shown in Figure 5.11, along with a plot of the model obtained from the Sigma Plot of $g(t)$ from the HSA recovery data in Figure 5.10. Normalizing the data with Equation (3.12) causes the signal at time $t = 0$ to become unity, and the increase in fluorescence is manifested as a decrease in $g(t)$. Despite the omission of the second exponential term, the equation fits the data well, especially at later times.

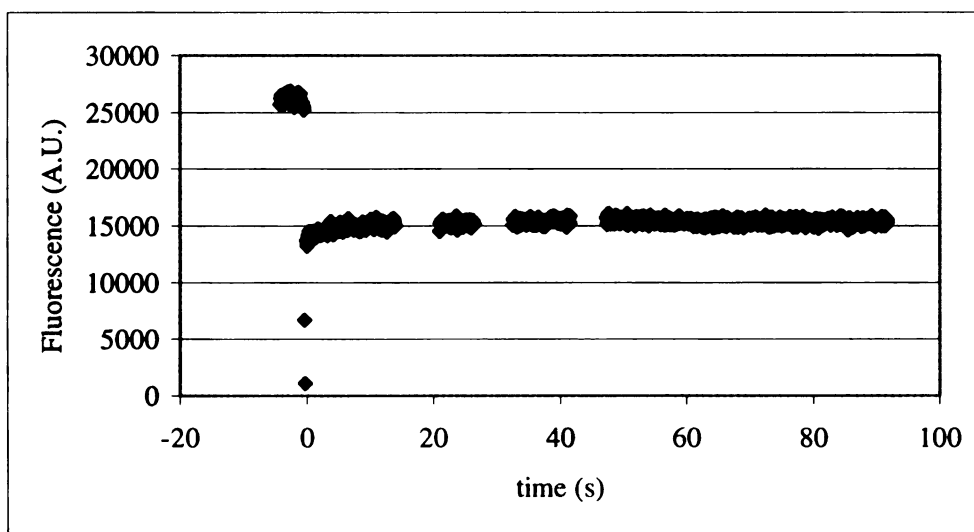


Figure 5.10: Sample fluorescence recovery curve for HSA adsorbed at an interface featuring a 6 μm oil layer. The fluorescence units are arbitrary (A.U.). The slow recovery of fluorescence after photobleaching is an indication that a large fraction of protein is bound irreversibly to the interface.

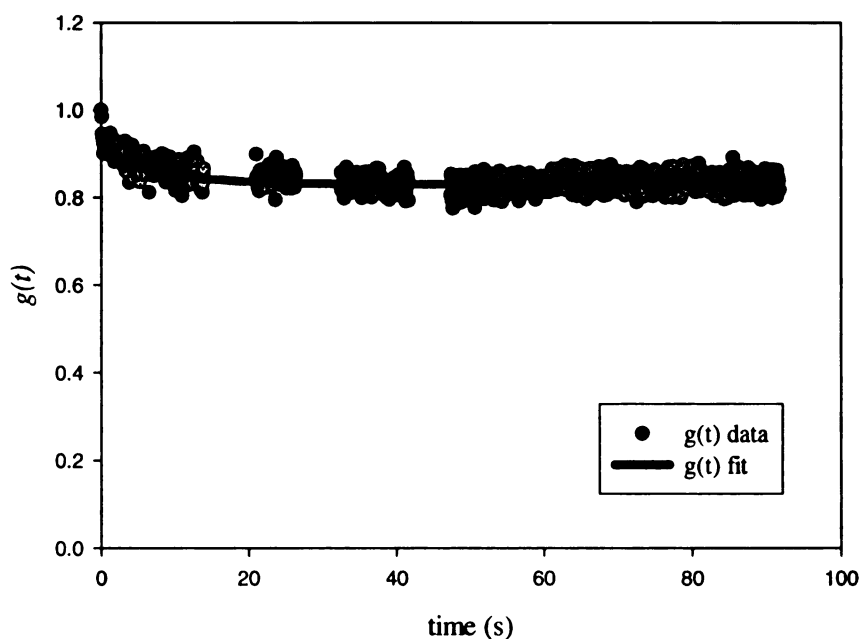


Figure 5.11: Sample $g(t)$ data and regression fit for HSA on 6 μm oil layer. $g(t)$ is normalized from the fluorescence recovery curve (Figure 5.10). The single exponential model fits the data well, even at later times.

The results of the TIRFM/FPR experiments with HSA at a concentration of 0.2 mg/ml are shown in Table 1. It was determined that this concentration was in the reaction limited regime, by experiment and by comparison with published reaction limited data of 0.1 mg/ml for BSA, a structurally and functionally similar protein³⁸. Experimental confirmation was obtained by comparing the results of a 0.7 mg/ml experiment to those of a 0.2 mg/ml experiment at the same oil layer thickness, and showing that they are statistically similar. This indicates that 0.2 mg/ml is within the reaction limit since an increase in protein concentration did not result in a change in the values determined for the constants in Equation (3.13).

In these experiments, oil layer thickness did not appear to influence the irreversibly bound fraction, g_0 , as would be expected. This would seem to indicate that there is a limit at which the thickness of the oil layer no longer plays a role in strengthening the interaction between the solid substrate and proteins bound at the liquid-liquid interface. That is, the stability conferred to the liquid-liquid interface by its proximity to the solid substrate has reached its maximum, and there is no further improvement in the interactions between the bound proteins and the substrate. Due to the viscosity of the oil, there is a limit to the thickness of the oil layer that can be attained in our system. In fact, 50 μm was the maximum thickness that could be reproducibly spin-coated on the microscope glass.

The oil layer thickness did not significantly affect g_1 , the fraction of proteins that constitutes the rapidly desorbing class, or $k_2(l)$, the desorption rate of the rapidly desorbing class of proteins (Table 1). There appears to be a difference in the $k_2(l)$ for the 50 μm oil layer. However, we believe this difference is more likely the result of photobleaching by the monitoring beam as the experiment progressed. The exponential parameters are greatly affected by data at longer adsorption timescales; therefore, photobleaching by the monitoring beam will have an impact on them.

The results of TIRFM/FPR experiments with fibronectin (FN) at a concentration of 0.05 mg/ml are shown in Table 2. As with HSA, g_0 did not depend on oil layer thickness. However, g_0 is higher for FN than for HSA. This is to be expected, since FN has been shown to be more aggressive at the oil-water interface than HSA³⁷. Vaidya and Ofoli³⁷ showed that FN has the ability to displace HSA at the liquid-liquid interface, even when

HSA has been pre-adsorbed at the interface for as long as six hours; on the other hand, HSA is unable to displace much FN from the interface.

Table 1: TIRFM/FPR results for HSA. Data are presented \pm the standard error from regression.

Thickness (μm)	g_0	g_1	$k_2(l)$
6	0.83 ± 0.001	0.10 ± 0.003	0.13 ± 0.009
12	0.84 ± 0.001	0.11 ± 0.006	0.14 ± 0.014
38	0.84 ± 0.001	0.09 ± 0.002	0.12 ± 0.006
50	0.85 ± 0.002	0.09 ± 0.012	0.31 ± 0.064

There is more variation in g_1 and $k_2(l)$ with thickness in the case of FN than was seen with HSA, with both g_1 and $k_2(l)$ increasing with increasing oil thickness. To understand the reasons for this, we should note that g_1 and $k_2(l)$ represent the fraction and desorption rate, respectively, of proteins in the rapidly desorbing class. Burghardt and Axelrod²⁵ discussed the possibility that the binding of proteins in this class may result from the formation of a monolayer of protein on a rough interface. It is possible that the interface may become rougher as the thickness of the oil layer increases, which could account for the increase in g_1 and $k_2(l)$. It is also possible that the concentration of FN in these experiments was on the edge of the reaction limited regime, and that the variations in g_1 and $k_2(l)$ are a result of this.

Table 2: TIRFM/FPR results for FN. Data are presented \pm the standard error from regression.

Thickness (μm)	g_0	g_1	$k_2(l)$
4	0.92 ± 0.0001	0.06 ± 0.0004	0.03 ± 0.0004
16	0.93 ± 0.0002	0.04 ± 0.0005	0.05 ± 0.0011
33	0.90 ± 0.0002	0.08 ± 0.0010	0.08 ± 0.0016

The results of the TIRFM/FPR experiments suggest that there is a point beyond which further decreases in the thickness of the oil layer do not affect protein adsorption at the liquid-liquid interface. On the other hand, the cell culture results show that cell growth and proliferation strongly depend on the fluorocarbon layer thickness. If improved cell growth is a function of better protein attachment, then the sigmoidal behavior presented in Figure 5.12 would be suggested by the TIRFM/FPR data, which show that there is no further improvement in protein layer stability at very thin oil layers.

Taken together, the two sets of data would strongly suggest the dashed line in Figure 5.12 as the most likely profile for cell growth with respect to fluorocarbon layer thickness. If, as the TIRFM/FPR data suggest, there is a point where making thinner FC-70 layers does not improve protein attachment at the liquid-liquid interface, and if cell growth at the liquid-liquid interface is affected by the strength of attachment of the underlying protein layer, then cell growth must indeed level off to some maximum asymptotic value at very thin fluorocarbon layers, as depicted in Figure 5.12.

Normal cell growth should not exceed the maximum number of cells that could be accommodated by the surface area of the vessel, because contact inhibition causes cells to cease proliferating once they are in contact with one another. This is true at the liquid-liquid interface as well. If the plastic surface is considered to have the maximum cell density available for the surface area of the culture vessel, then as the fluorocarbon layer gets thinner, cell growth should approach this maximum number of cells. As the thickness of the fluorocarbon layer approaches zero, cell growth should level off towards

the maximum allowed by the surface area of the culture plate, since 3T3 cells are contact-inhibited³⁹.

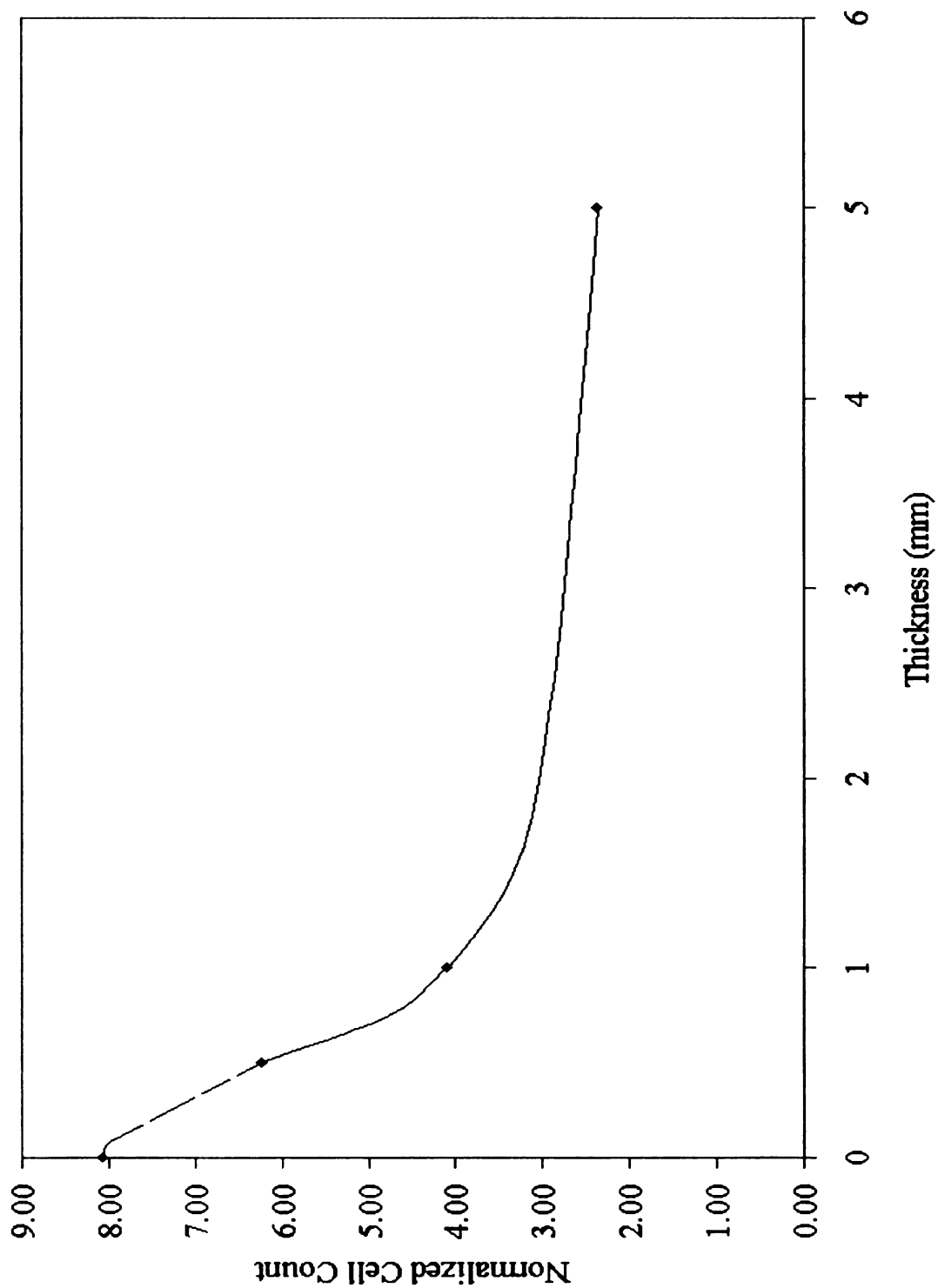


Figure 5.12: Most likely cell growth curve as a function of fluorocarbon layer thickness for FN on Day 3. The dashed line represents the most plausible cell growth profile, based on the combination of results from TIRFM/FPR and cell culture experiments.

6. SUMMARY AND CONCLUSIONS

Cell culture at a liquid-liquid interface provides an alternative to cell culture on a solid substrate, and eliminates some of the problems commonly associated with a solid substrate. It is generally believed that a liquid-liquid interface is more uniform than a solid substrate¹². Cells can be removed from a liquid-liquid interface without the use of damaging treatments such as application of trypsin-EDTA or scraping. There are, however, some drawbacks to cell culture at the liquid-liquid interface. Chief among them is the breakage of the layer of protein that adsorbs at the interface and supports cell growth. When this happens, it causes cells to form aggregates and large cell-free open areas commonly referred to as “lakes.” In this work, it was hypothesized that decreasing the thickness of the underlying fluorocarbon layer would provide a solution to this problem, because it would impart more interfacial stability and improve the anchorage of proteins at the interface. This should decrease the incidence of protein layer rupture and lead to improved cell growth and proliferation.

The objective of this work, therefore, was to study the effect of fluorocarbon layer thickness on the adsorption of human serum albumin (HSA) and fibronectin (FN) at the liquid-liquid interface, and assess the influence of fluorocarbon layer thickness on the attachment and growth of cells cultured at the interface. Cell attachment and growth at the interface between culture medium and FC-70 layers of 5 mm, 1 mm, and 0.5 mm were measured, with either FN or HSA preadsorbed at the interface. The adsorption and reversibility of HSA and FN was examined directly by total internal reflection fluorescence microscopy (TIRFM) on oil layers ranging in thickness from 4 μm to 50 μm .

Cell attachment and growth were clearly influenced by the thickness of the FC-70 layer. Growth and proliferation improved as the fluorocarbon layers became thinner, with the best growth on the 0.5 mm thick layer. Cells were also more densely packed on the 0.5 mm layer than on the 1 mm and 5 mm ones. There were larger cell free gaps on the 1 mm and 5 mm thick layers and more aggregates formed, indicating that the layers of adsorbed protein had ruptured more on the thicker fluorocarbon layers than on the thinnest one. This is most likely because the thinner fluorocarbon layers promote interfacial stability of the adsorbed protein layer, facilitating better cell attachment, growth and proliferation, and diminishing protein layer breakage, as was hypothesized in this study.

The type of protein adsorbed at the liquid-liquid interface also influenced the growth of cells. While cell growth improved as the thickness of the fluorocarbon layer decreased for both proteins, cells grew much better on FN-treated interfaces than on HSA-treated ones. In all cases, cell numbers were typically higher for FN-treated interfaces over the culture period. FN-treated interfaces had larger areas of densely packed cells on both the 0.5 mm and 1 mm thick layers. More aggregates formed on HSA-treated interfaces and there were larger areas with no cell growth.

An interesting problem was encountered when cells were removed from the interface. Based on the assumption that cells do not adhere as strongly to the liquid-liquid interface, it was hypothesized that trypsin-EDTA treatment would lead to total removal of cells from the interface. However, trypsin-EDTA alone was not enough to remove all of the

cells. In some cases, no cells were removed at all following treatment with trypsin-EDTA, especially from FN-treated interfaces. Normally, cells should be rounded up and ready to be detached after about 20 minutes of treatment by trypsin-EDTA. Results in this study showed that, after treatment, cells on HSA-treated FC-70 and on bare plastic had rounded up and were apparently ready to be removed. However, on FN-treated interfaces, the cells were still spread out and were clearly not ready for removal. Therefore, it was necessary to scrape the interfaces to detach the cells.

Protein adsorption at the liquid-liquid interface was studied by TIRFM/FPR, with oil layers ranging from 4 μm to 50 μm thick. In these experiments, oil layer thickness did not significantly influence g_0 , the fraction of protein irreversibly bound at the interface, which was taken to be an indicator of the strength of the adsorbed protein layer, for both HSA and FN. In all cases, g_0 was greater for FN than for HSA. For HSA, the rapidly desorbing fraction of protein, g_1 , and its desorption rate, $k_2(1)$, did not vary with thickness either. On the other hand, both g_1 and $k_2(1)$ for FN did vary with oil layer thickness.

The TIRFM/FPR results for both proteins show that there is no difference in the fraction of proteins irreversibly adsorbed at the interface for oil layers ranging from 4 to 50 μm . This would suggest that, within 50 μm of the interface, oil layer thickness has no effects on protein adsorption at the liquid-liquid interface. Therefore, cell attachment and proliferation could not be further improved, except for the responses of the cells to different proteins adsorbed at the interface. On the other hand, the cell culture results show that, down to a thickness of 0.5 mm, cell growth and proliferation strongly depend

on the thickness of the fluorocarbon layer for a given protein. If, as hypothesized, improved cell growth is a function of the strength or quality of the adsorbed protein layer, then these data together would suggest a sigmoidal behavior for cell growth at the liquid-liquid interface, with cell growth leveling off asymptotically to some maximum value as the thickness of the fluorocarbon layer decreases.

7. SUGGESTIONS FOR FUTURE WORK

1. Among the studies total internal reflection fluorescence has been used for is visualization of cell-substrate contact regions²⁰. The degree of cell adhesion to a substrate can be studied and the strength of cellular adhesion can be inferred from the number of focal contacts⁴⁰. The current TIRFM apparatus can be adapted to study cells cultured at the liquid-liquid interface. Such studies would provide further confirmation of the hypothesis.
2. To further verify our results, it would be useful to examine cell growth on even thinner fluorocarbon layers. This may be achieved by looking into the use of other fluorocarbons, which may not show the same effects as FC-70, HFE-7100, and HFE-7500. Alternatively, the cell culture plates may be treated with something, like photoresist, to make them more hydrophobic. There are drawbacks to treating the culture plates with other chemicals, as they may be toxic to the cells and are not necessarily sterile. Another option would be to try bacteriological culture plates, which are treated to by hydrophobic.
3. Different cell types behave differently when cultured at the liquid-liquid interface. Repeating these experiments with a different cell line, such as HeLa cells, may provide further verification of the thickness results.
4. Atomic force microscopy (AFM) is a valuable tool for studying protein configuration and attachment and cell attachment on surfaces. AFM is being

adapted to the study of liquid-liquid interfaces⁴¹⁻⁴³. In the future, AFM may be useful for studying protein adsorption and cells cultured at the liquid-liquid interface, providing information on the conformation of protein adsorbed at the interface as well as the strength of cellular attachment at the interface.

8. APPENDICES

8.1 Appendix A: Physical Properties of FC-70

FC-70 is a clear, colorless liquid comprised of a mixture of fully-fluorinated compounds that are blended to achieve specific physical properties.

Table 3: Physical properties of FC-70. Values are determined at 25 °C.

Properties	
Average Molecular Weight	820
Boiling Point (1 atm)	215 °C
Liquid Density	1940 kg/m ³
Absolute Viscosity	24 cp
Surface Tension	18 dynes/cm

8.2 Appendix B: Sigma Plot Output

A sample of the output from Sigma Plot for the determination of the parameters in Equation (3.13) from fluorescence recovery data is given below. Initial guesses for the coefficients were provided to the regression program, and then the resulting solutions were input back into the program as new initial guesses until the percent variance was minimized.

[Variables]

t=col(1)

y=col(2)

[Parameters]

g0 = 0.75 ' {{previous: 0.829841}}

g1 = 0.25 ' {{previous: 0.0883611}}

k1 = 1.2 ' {{previous: 0.0968088}}

[Equation]

f=g0+g1*exp(-k1*t)

fit f to y

[Constraints]

k1>0

g1>0

g0>0

[Options]

tolerance=0.000100

stepsize=100

iterations=100

R = 0.5081 Rsqr = 0.2582 Adj Rsqr = 0.2549

Standard Error of Estimate = 0.0419

	Coefficient	Std. Error	t	P
g0	0.8298	0.0049	169.8753	<0.0001
g1	0.0884	0.0073	12.0816	<0.0001
k1	0.0968	0.0238	4.0674	<0.0001

Analysis of Variance:

	DF	SS	MS	F	P
Regression	2	0.2729	0.1364	77.7896	<0.0001
Residual	447	0.7840	0.0018		
Total	449	1.0569	0.0024		

PRESS = 0.7951

Durbin-Watson Statistic = 1.8886

Normality Test: K-S Statistic = 0.0349 Significance Level = 0.6351

Constant Variance Test: Passed (P = 0.5840)

Power of performed test with alpha = 0.0500: 1.0000

9. BIBLIOGRAPHY

1. Freshney, R. I. *Culture of Animal Cells: a manual of basic techniques* (Wiley, New York, 2000).
2. Rosenberg, M. D. in *Cellular Control Mechanisms and Cancer* (eds. Emmelot, P. & Muhlbock, O.) 146-164 (Elsevier, New York, 1964).
3. Shiba, Y., Ohshima, T. & Sato, M. Growth and morphology of anchorage-dependent animal cells in a liquid/liquid interface system. *Biotechnology and Bioengineering* **57**, 583-589 (1998).
4. Rappaport, C. et al. New perfluorocarbon system for multilayer growth of anchorage-dependent mammalian cells. *Biotechniques* **32**, 142- (2002).
5. Lowe, K. C. Perfluorochemical respiratory gas carriers: benefits to cell culture systems. *Journal of Fluorine Chemistry* **118**, 19-26 (2002).
6. Keese, C. R. & Giaever, I. Cell growth on liquid interfaces : Role of surface active compounds. *Proceedings of the National Academy of Sciences of the United States of America-Biological Sciences* **80**, 5622-5626 (1983).
7. Giaever, I. & Keese, C. R. Behavior of cells at fluid interfaces. *Proceedings of the National Academy of Sciences of the United States of America-Biological Sciences* **80**, 219-222 (1983).
8. Hynes, R. O. *Fibronectins* (Springer-Verlag, New York, 1990).
9. Turner, M. W. & Hulme, B. *The Plasma Proteins* (Pitman Medical & Scientific Publishing Co. Ltd., London, 1971).
10. Groth, T., Altankov, G. & Klosz, K. Adhesion of human peripheral-blood lymphocytes is dependent on surface wettability and protein preadsorption. *Biomaterials* **15**, 423-428 (1994).

11. Packham, M. A., Evans, G., Glynn, M. F. & Mustard, J. F. The effect of plasma proteins on the interaction of platelets with glass surfaces. *Journal of Laboratory and Clinical Medicine* **73**, 686-697 (1969).
12. Ando, J., Albelda, S. M. & Levine, E. M. Culture of human adult endothelial cells on liquid-liquid interfaces: A new approach to the study of cell-matrix interactions. *In Vitro Cellular & Developmental Biology* **27**, 525-532 (1991).
13. Keese, C. R. & Giaever, I. Substrate mechanics and cell spreading. *Experimental Cell Research* **195**, 528-532 (1991).
14. Sparrow, J. R., Ortiz, R., MacLeish, P. R. & Chang, S. Fibroblast behavior at aqueous interfaces with perfluorocarbon, silicone, and fluorosilicone liquids. *Investigative Ophthalmology & Visual Science* **31**, 638-646 (1990).
15. Kwon, Y. J., Yu, H. & Peng, C. A. Enhanced retroviral transduction of 293 cells cultured on liquid-liquid interfaces. *Biotechnology and Bioengineering* **72**, 331-338 (2001).
16. Terada, S., Sato, M., Katayama, R. & Shinozawa, T. Recovery of intact membrane proteins from adherent animal cells grown in a liquid-liquid interface. *Journal of Fermentation and Bioengineering* **74**, 330-332 (1992).
17. Sobel, S. & Rosenberg, M. D. Characterization of cellular attachment and spreading molecules at liquid-liquid interfaces. *Analytical Biochemistry* **140**, 486-489 (1984).
18. Rappaport, C., Trujillo, E. M. & Soong, L. F. Novel oxygenation system supports multilayer growth of HeLa cells. *Biotechniques* **21**, 672-677 (1996).
19. Axelrod, D., Hellen, E. H. & Fulbright, R. M. in *Topics in Fluorescence Spectroscopy* (ed. Lakowicz, J. R.) 289-343 (Plenum Press, New York, 1992).
20. Axelrod, D. in *Methods in Enzymology: Biophotonics Part B* (eds. Marriot, G. & Parker, I.) 1-33 (Academic Press, New York, 2003).
21. Conboy, J. C., McReynolds, K. D., Gervay-Hague, J. & Saavedra, S. S. Quantitative measurements of recombinant HIV surface glycoprotein 120 binding

- to several glycosphingolipids expressed in planar supported lipid bilayers. *Journal of the American Chemical Society* **124**, 968-977 (2002).
22. Hlady, V. & Ho, C. H. Human low density lipoprotein (LDL) and human serum albumin (HSA) co-adsorption onto the C18-silica gradient surface. *Materialwissenschaft und Werkstofftechnik* **32**, 185-192 (2001).
 23. Hashimoto, F., Tsukahara, S. & Watarai, H. Lateral diffusion dynamics for single molecules of fluorescent cyanine dye at the free and surfactant-modified dodecane-water interface. *Langmuir* **19**, 4197-4204 (2003).
 24. Thompson, N. L., Burghardt, T. P. & Axelrod, D. Measuring surface dynamics of biomolecules by total internal reflection fluorescence with photobleaching recovery or correlation spectroscopy. *Biophysical Journal* **33**, 435-454 (1981).
 25. Burghardt, T. P. & Axelrod, D. Total internal reflection fluorescence photobleaching recovery study of serum albumin adsorption dynamics. *Biophysical Journal* **33**, 455-467 (1981).
 26. Huang, C. Z., Lu, W. & Li, Y. F. Analytical applications of resonance light-scattering signals totally reflected at liquid/liquid interface. *Reviews in Analytical Chemistry* **21**, 267-278 (2002).
 27. Gajraj, A. & Ofoli, R. Y. Quantitative technique for investigating macromolecular adsorption and interactions at the liquid-liquid interface. *Langmuir* **16**, 4279-4285 (2000).
 28. Gajraj, A. & Ofoli, R. Y. Effect of extrinsic fluorescent labels on diffusion and adsorption kinetics of proteins at the liquid-liquid interface. *Langmuir* **16**, 8085-8094 (2000).
 29. Jones, M. A. & Bohn, P. W. Total internal reflection fluorescence and electrocapillary investigations of adsorption at a H₂O-dichloroethane electrochemical interface. 1. Low-frequency behavior. *Analytical Chemistry* **72**, 3776-3783 (2000).
 30. Jones, M. A. & Bohn, P. W. Total internal reflection fluorescence and electrocapillary investigations of adsorption at the water-dichloroethane electrochemical interface. 2. Fluorescence-detected linear dichroism investigation

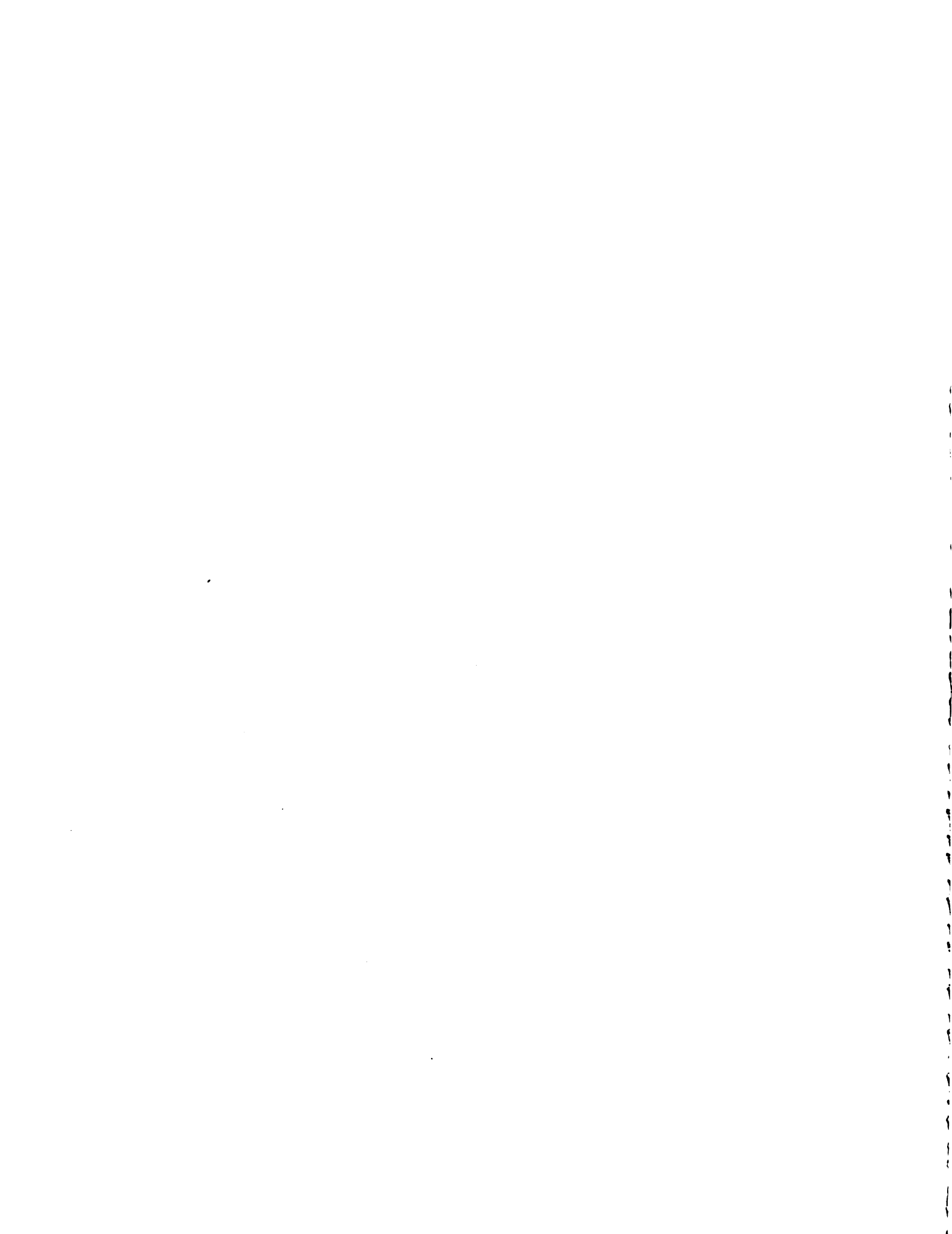
of adsorption-driven reorientation of di-N-butylaminonaphthylethylenylpyridinium-propylsulfonate. *Journal of Physical Chemistry B* **105**, 2197-2204 (2001).

31. Ishizaka, S., Kim, H. B. & Kitamura, N. Time-resolved total internal reflection fluorometry study on polarity at a liquid/liquid interface. *Analytical Chemistry* **73**, 2421-2428 (2001).
32. Yamashita, T., Uchida, T., Fukushima, T. & Teramae, N. Solvation dynamics of fluorophores with an anthroyloxy group at the heptane/water interface as studied by time-resolved total internal reflection fluorescence spectroscopy. *Journal of Physical Chemistry B* **107**, 4786-4792 (2003).
33. Feng, P., Li, Y. F. & Huang, C. Z. Determination of chlortetracycline in body fluids with the complex cation of chlortetracycline-europium(III)-trioctylphosphine oxide by total internal reflected fluorescence at a water/tetrachloromethane interface. *Analytica Chimica Acta* **442**, 89-95 (2001).
34. Feng, P., Huang, C. Z. & Li, Y. F. Determination of berberine by measuring the enhanced total internal reflected fluorescence at water/tetrachloromethane interface in the presence of sodium dodecyl benzene sulfonate. *Analytical and Bioanalytical Chemistry* **376**, 868-872 (2003).
35. Feng, P., Huang, C. Z. & Li, Y. F. Direct quantification of human serum albumin in human blood serum without separation of gamma-globulin by the total internal reflected resonance light scattering of thorium-sodium dodecylbenzene sulfonate at water/tetrachloromethane interface. *Analytical Biochemistry* **308**, 83-89 (2002).
36. *Amine-Reactive Probes* (Molecular Probes, Eugene, OR, 2003).
37. Vaidya, S. & Ofoli, R. Y. Adsorption of human plasma fibronectin at the oil-water interface: A competitive adsorption study. *Langmuir* (Submitted 2003).
38. Chan, V., Graves, D. J., Fortina, P. & McKenzie, S. E. Adsorption and surface diffusion of DNA oligonucleotides at liquid/solid interfaces. *Langmuir* **13**, 320-329 (1997).
39. Jainchill, J. L., Aaronson, S. A. & Todaro, G. J. Murine sarcoma and leukemia viruses: assay using clonal lines of contact-inhibited mouse cells. *Journal of Virology* **4**, 549-553 (1969).

40. Burmeister, J. S., Olivier, L. A., Reichert, W. M. & Truskey, G. A. Application of total internal reflection fluorescence microscopy to study cell adhesion to biomaterials. *Biomaterials* **19**, 307-325 (1998).
41. Chan, D. Y. C., Dagastine, R. R. & White, L. R. Forces between a rigid probe particle and a liquid interface - I. The repulsive case. *Journal of Colloid and Interface Science* **236**, 141-154 (2001).
42. Dagastine, R. R. & White, L. R. Forces between a rigid probe particle and a liquid interface - II. The general case. *Journal of Colloid and Interface Science* **247**, 310-320 (2002).
43. Nespolo, S. A., Chan, D. Y. C., Grieser, F., Hartley, P. G. & Stevens, G. W. Forces between a rigid probe particle and a liquid interface: Comparison between experiment and theory. *Langmuir* **19**, 2124-2133 (2003).

9.1 General References

1. *Basic Cell Culture: A Practical Approach* (ed. Davis, J. M.) (Oxford University Press, New York, 2002).
2. Harrison, M. A. & Rae, I. F. *General Techniques of Cell Culture* (Cambridge University Press, New York, 1997).
3. Martin, B. M. *Tissue Culture Techniques: An Introduction* (Birkhauser, Boston, 1994).



MICHIGAN STATE UNIVERSITY LIBRARIES



3 1293 02504 7204